The Greek Database of Seismogenic Sources (GreDaSS): state-of-the-art for northern Greece.

Caputo R.*, Chatzipetros A.°, Pavlides S.° and Sboras S.*

*) Department of Earth Sciences, University of Ferrara, Italy

°) Department of Geology, Aristotle University of Thessaloniki, Greece

Abstract

The Greek Database of Seismogenic Sources (GreDaSS) is a repository of geological, tectonic and active fault data for the Greek territory and its surroundings. In this paper, we present the state-of-the-art of an on-going project devoted to the building of GreDaSS, which represents the results of decades of investigations by the authors and a myriad of other researchers working on the active tectonics of the broader Aegean Region. The principal aim of this international project is to create a homogenized framework of all data relevant to the seismotectonics, and especially the seismic hazard assessment, of Greece and its surroundings as well as a common research platform for performing seismic hazard analyses, modelling and scenarios from specific seismogenic structures. In particular, we introduce and synthetically describe the results obtained (and included in the database) up to date relative to the northern sector of continental Greece and Aegean Sea. As a first step we collected all available data (both published and unpublished) relative to the historical and instrumental seismicity determining the causative faults. Following the experience of recent 'surprising' earthquakes (*e.g.* 1995 Kozani and 1999 Athens), we realized the deficiency of such approach and decided to include in GreDaSS also active faults (*i.e.* seismogenic sources) recognized on the basis of geological, structural, morphotectonic, palaeoseismological and geophysical investigations. A second step is represented by the critical analysis of all collected data for extracting the necessary seismotectonic information enabling the recognition of as many as possible seismogenic sources as well as their characterization and parameterization. The most updated version of the database consists of numerous seismogenic sources categorized in three types: composite (CSS), individual (ISS) and debated (DSS). The amount of information and the degree of uncertainty is different for the three types.

keywords: North Aegean, seismotectonics, earthquake geology, active faults

1. Introduction

The Aegean Region is characterized by intense seismicity both in terms of magnitude and frequency. Although shallow earthquakes in Greece commonly occur along well defined zones (*e.g.* Gulf of Corinth, South Thessaly, Ionian Sea), moderate to strong events have also occurred in areas where seismicity was considered very low or totally absent (*e.g.* Kozani and Athens as the two most recent examples). Thus, seismic hazard could not be estimated only from historically or instrumentally well known sources (Pavlides and Caputo, 2004). Earthquakes have caused many casualties in both human lives and constructions in Greece since the early known historical events (*e.g.* Papazachos and Papazachou, 1997, Papadopoulos, 2000). The seismic risk nowadays is even greater than in the past due to much denser population, living in big cities characterized by a higher building complexity. A representative example is the September 7, 1999 (M_s = 5.9) Athens earthquake, which even though it was a moderate event, it strongly affected the urban metropolitan area of Athens, which accommodates nearly half of the Greek population, causing many deaths and severe damage. Previously, the area was considered of low seismic activity, since no important earthquakes were reported either historically or instrumentally (Papadimitriou *et al.*, 2002), and the causative Fili Fault (Pavlides *et al.*, 2002), which has a clear morphotectonic expression (Ganas *et al.*, 2004), was not recognized as an active fault until then. Another, even more striking example is represented by the 1995 Kozani earthquake which occurred in an area previously considered aseismic.

Therefore, the recognition of active faults and their seismotectonic characterization with other non-seismological tools are crucial steps for contributing to the seismic hazard assessment of a highly seismogenic region like Greece. At this regard, active faults are often studied individually or at a regional scale. This causes two effects: firstly, data are scattered and sometimes "hidden" in various studies and secondly data are sometimes inconsistent when they derive from investigations carried out by different approaches and different authors.

Having foreseen the importance to hold and manage all collected data from active fault investigations, many research institutes worldwide have built databases at the national scale. For example, the Geological National Survey in New Zealand (GNS; http://data.gns.cri.nz/af/), the Institute of Advanced Industrial Science and Technology in Japan (AIST; http://riodb02.ibase.aist.go.jp/activefault/index_e.html), the Geological Survey in the United States (USGS; http://pubs.usgs.gov/fs/2004/3033/fs-2004-3033.html) and the Istituto Nazionale di Geofisica e Volcanologia in Italy (INGV; http://diss.rm.ingv.it/diss/) have certainly the most developed databases of active faults. Following the track, but especially feeling the need to fill a scientific gap, we are currently building a similar database for the Aegean region, the *Greek Database of Seismogenic Sources* (GreDaSS). It is a continuously updatable database of all faults reactivated in historical or instrumental times as well as of geologically determined active and capable faults (Fig. 1). The database provides many levels of consistent and uniform information, like the principal

seismotectonic parametres (*e.g.* location, geometry, kinematics *etc*.), descriptions (comments, open questions and literature summaries, figures, relevant literature, *etc.*) and much more.

The informatic structure and methodological approach of GreDaSS is based on the well tested, time-proof, worldwide acknowledged database proposed by the INGV for the Italian Database of Individual Seismogenic Sources (DISS), which represents the result of almost twenty years research experience of its Working Group (Valensise and Pantosti, 2001; Basili *et al.*, 2008). It is built in a GIS environment, containing all necessary geographical information, for the appropriate representation, and all available structural parameters accompanied with comments, open questions, short summaries of the available literature and selected figures. Seismogenic sources consist of three main categories: Individual Seismogenic Sources (ISSs), Composite Seismogenic Sources (CSSs) and Debated Seismogenic Sources (DSSs). This paper is not focused on the description of the philosophy, structure and technical issues of the database; the corresponding information can be found in Basili *et al.* (2008). On the other hand, the principal aim of this paper is to present the state-of-the-art of GreDaSS by synthetizing all seismogenic sources included in northern Greece as far as this region is satisfactorily complete. The investigations for other sectors of the Aegean are still in progress and will be not presented and discussed here.

It is important to remind that four parameters (length, width, slip-per-event and magnitude) of the ISSs are interconnected by seismological scaling relationships (Kanamori and Anderson, 1975; Hanks and Kanamori, 1979, Wells and Coppersmith, 1994; Pavlides and Caputo, 2004). Thus, if not all of four parameters are known, they can be estimated accordingly. The approach is slightly different for the CSSs, because they show more complexity in terms of segmentation. For this reason, the potential magnitude is inferred, after taking into account geological considerations.

All segments of limited dimensions, thus not capable of producing at least a moderate earthquake, are deliberately excluded from the database. On the other hand, ISSs may consist of smaller geological segments which can be briefly described through the ISS properties. A CSS can also consist of many ISSs characterized as segments. In this case, an ISS is defined as a portion of a greater structure showing an individual seismotectonic behaviour in the recent past. This does not exclude that the segment is presently breached with nearby segments or that the segments seismically behave as a unique rupture surface or will seismically behave as a unique seismogenic source in the future. For this reason the likelihood that a single event will occur reactivating either breached, linked or yet isolated segments is discussed for each CSS.

2. Building the database

For constructing any database of seismogenic sources, there are two basic steps: firstly, all active faults affecting a specific region should be recognized and, secondly, each seismogenic structure should be seismotectonically parameterized. In order to achieve the first step, especially in regions like the Aegean, where earthquake catalogues cover a very long time period (*ca.* 2500 years), are particularly rich and relatively complete at least as concern the major events, it is common practice to start analyzing the historical and instrumental seismicity affecting the specific region. In particular, major events are systematically considered and tentatively associated with the specific causative fault (Fig. 2).

However, seismicity in Northern Greece is not homogeneously distributed, neither in frequency nor in density. Historical information is similarly not uniform all over the region and even the most complete and updated earthquake catalogues (Ambraseys and Jackson, 1990; 1998; Guidoboni *et al.*, 1994; Papazachos and Papazachou, 1997; 2003; Guidoboni and Comastri, 2005; Ambraseys, 2001; 2009) are in some case contradicting or doubtful in describing past events, especially the older ones, thus hampering a quantitative exploitation of the data and making sometimes hard the correlation of the events with any recognized fault (Caputo *et al.*, 2008). For example, a quick view of the entire study area shows a sparse and infrequent seismicity in Eastern Macedonia and Thrace Region, where no significant seismicity is instrumentally recorded. On the contrary, Central Macedonia and Chalkidiki show intense activity including instrumentally recorded events (*e.g.* the 1932, Ierissos and the 1978, Thessaloniki earthquakes) and plenty records of historic events. West Macedonia was demonstrating extremely low seismicity (Voidomatis, 1989; Papazachos, 1990) until May 15, 1995, when an M_w = 6.5 earthquake occurred in the vicinity of Kozani. The pattern changes back to sparse and infrequent seismicity with few instrumentally recorded moderate events in the area of Epirus and generally the broader Northwestern Greece. A possible explanation for this difference is that the historical record is obviously richer in densely populated areas, while mountainous regions like Epirus were always sparsely populated. Nevertheless, also instrumental seismicity seems to verify this difference, although the time window is too narrow.

Following the above criticisms and due to the associated uncertainties, any database of seismogenic sources ensued only on historical and instrumental seismicity would be largely incomplete and therefore of limited use, for example, for seismic hazard assessment analyses. Accordingly, we decided to include in GreDaSS also seismogenic sources recognized on the basis of other criteria and use the available data to improve the seismotectonic parameterization of the 'historically'-related sources (see discussion in Caputo *et al.*, 2008). In other terms, all seismogenic sources included in the database have been recognized, selected and seismotectonically characterized by appropriately blending the information obtained from the different approaches, methods and

investigation techniques like instrumental, historical, palaeoseismological and morphotectonic, but sometimes also archaeoseismological or geodetic, and this has been opportunely weighted according to the degree of uncertainty attributed to each single available information.

In figure 1 are represented all the seismogenic sources (either CSS and ISS) included at present in GreDaSS roughly north of the latitude 39°N. At a first glance of the figure, the CSSs and ISSs that affect this region roughly delineate five sectors: i) a northern E-W trending fault belt in Thrace and Eastern Macedonia, ii) a complex E(SE)-W(NW) trending fault system affecting the Chalkidiki peninsula and possibly associated with low-angle detachments, iii) the NE-SW trending transverse anti-orogenic ('anti-Hellenides') fault system in Western Macedonia and Epirus, iv) the (E)NE-(W)SW trending North Aegean fault system, which is almost exclusively located offshore, and v) the E(SE)-W(NW) trending Thessalian fault system. In the following chapters all seismogenic sources are synthetically described in terms of seismotectonic parameters and their relation with historical and instrumental earthquakes is discussed. In contrast, the DSSs represented in Fig. 1 will be not described and discussed in this paper.

3. The northern Greece fault belt

Northern continental Greece, and particularly Thrace and Eastern Macedonia are affected by several roughly E-W trending normal faults forming an almost continuous regional-scale fault belt extending for more than 300 km starting from the border with Turkey to the Vardar Valley. In the database are included five CSSs some of which also contain well recognized segments (ISSs).

Some historical seismic events, among which are the Komotini 1784, Drama 1829 and Xanthi 1829, occurred in this region and are discussed in the following together with the causative faults. However, no moderate-to-strong earthquakes hit the area since then and certainly not during the instrumental period.

3.1. Maronia CSS

The Maronia CSS is a *ca.* 54 km-long fault zone, striking E-W to ESE-WNW and dipping to the south (Fig. 3; Chatzipetros and Pavlides, 2004; Mountrakis *et al.*, 2006). Chatzipetros and Pavlides (2004) recognize three segments. i) The Marmaritsa Fault, to the west strongly controls the shoreline by creating an impressive N110°-120° striking scarp associated with a southwards dipping (55°-60°) fault. This segment is characterised by an up to 5 m-thick brecciation zone, showing evidence of recent reactivations (corrugations, striations, *etc*.). ii) The central Messimvria Fault, striking E-W and dipping southwards (70°-75°) mainly extends offshore and is based on bathimetry. iii) The eastern Makri Fault, partially overlapping the Messimvria Fault, is associated with a group of minor south-dipping sliding planes affecting young (Late Quaternary?) sediments and elongated marine terraces. The latter is the most active segment among the three, but the dimensions are not sufficient to produce at least an intermediate event (M>5.5), and therefore they have been not included in the database as ISSs. It is also worth mentioning that the behaviour and interaction of the segments have not been sufficiently investigated.

To the west, the Maronia CSS possibly continues offshore as suggested by bathymetric maps, while to the east a microseismic sequence of June and July, 2004 (Kiratzi *et al.*, 2005) as well as some morphological evidence suggest that the fault probably extends eastwards to the Evros Valley. By applying the empirical relationships between magnitude and length (Pavlides and Caputo, 2004) to the total length of the CSS, the maximum expected magnitude is *ca.* 7.0, which certainly represents the worst case scenario.

3.2. Thrace CSS (Komotini, Iasmos and Xanthi ISSs)

This S-dipping tectonic structure, probably more than 120 km-long, separates the Rhodope Mountain, to the north, from the Kavala-Xanthi-Komotini basin, to the south (Fig. 3). The strike of the fault trace varies from 40° to 115° forming important angular bends. Extensional faulting is active since at least Miocene bearing striations of three tectonic phases (Lybéris, 1984; Lybéris and Sauvage,

1985). The trace has been well mapped by several researchers (Lybéris, 1984; Mountrakis and Tranos, 2004; Rondoyanni *et al.*, 2004). Based on sea bottom seismic reflection profiles (Martin, 1987), the structure likely continues offshore westwards within the Gulf of Kavala.

This CSS is divided in four major segments (Mountrakis and Tranos, 2004; Mountrakis *et al.*, 2006), but only the three eastern ones show clear morphological evidence of recent activity and they have been classified as distinct ISSs: *Komotini*, *Iasmos* and *Xanthi* (from east to the west, respectively). The fault barriers between segments are of angular type producing differences in strike and dip and generating an overall zig-zag geometry. The dip-angle seems to progressively decrease towards the west (Mountrakis and Tranos, 2004; Mountrakis *et al.*, 2006; Rondoyanni *et al.*, 2004). This probably implies that maximum depth of the fault zone also progressively decreases westwards. The measured slip vectors indicate a generally dip-slip normal kinematics, though oblique-slip displacements locally prevail (Lybéris, 1984; Mountrakis and Tranos, 2004; Mountrakis *et al.*, 2006; Rondoyanni *et al.*, 2004). Slip-per-event for each fault segment ranges from 0.55 to 0.90 m. Taking into account the characteristics of the geometrical barriers and assuming the possibility of a dynamic triggering model, the worst case scenario implies the contemporaneous rupture of more than one segment. The 'softest' (*i.e.* the easiest to break during an earthquake) barrier is probably the one between the Xanthi and Iasmos segments which some authors already describe as a unique structure (Lybéris, 1984; Rondoyanni *et al.*, 2004). Assuming 44 km of total length, the empirical relationships (Pavlides and Caputo, 2004), indicate a maximum expected magnitude of 7.0.

The Komotini ISS has been tentatively associated with the 1784, November 6 earthquake (Papazachos and Papazachou, 1997; Mountrakis *et al.*, 2006), though the estimated magnitude (6.7; Papazachos and Papazachou, 1997) could be much lower (*e.g.* Ambraseys, 2009). Also the more recent 1829, April 11, Xanthi earthquake is lively debated. Indeed, Papazachos and Papazachou (1997) consider it as a foreshock of the May 5, 1829 Drama earthquake (see Drama CSS below), while the description in Ambraseys (2009) suggests that the area near Xanthi town mainly ruined, in contrast with the area surrounding Drama that was mostly damaged by the second event. If this is the case, it would imply that April 11 earthquake was not a foreshock of the same seismogenic source, but a distinct event that probably triggered the Drama earthquake *ca* one month later. Accordingly, the April 11, 1829 earthquake has been associated with the Xanthi ISS.

3.3. Drama CSS (Prosotsani and Drama ISSs)

This is a *ca.* 48 km-long fault zone, trending E-W, bounding to the north the Drama Basin and consisting of two segments: *Prosotsani* and *Drama* ISSs (Fig. 3). Both segments are distinguished based on detailed morphotectonic mapping (Mountrakis *et al.*, 2006) and show a right-stepping geometry with a significant overlap. Most geometric and kinematic parameters proposed by the same authors are in agreement with the focal mechanism of a moderate event (M_w = 5.2) that occurred on November 9, 1986 (Dziewonski *et al.*, 1986; Vannucci and Gasperini, 2003; 2004). In particular,

where the overlap occurs both segments probably join at depth into a single shallow-angle fault plane. Slip-per-event for each fault segment ranges from 0.50 to 0.7 m.

Papazachos and Papazachou (1997) refer to the 1829, May 5, Drama earthquake as a catastrophic event with a magnitude of 7.3, which is likely overestimated due to the occurrence of the strong nearby April 11 earthquake (see discussion in Thrace CSS, §3.2). The May 5 event has been associated with the Drama CSS (Mountrakis *et al.*, 2006), but not to any of the two segments. Taking into account the total length of the CSS, a maximum expected magnitude of 7.0 is proposed (Pavlides and Caputo, 2004), confirming the overestimate of the 1829 Drama earthquake.

3.4. Serres CSS

Also this fault zone has a S-dipping setting showing a slight curvature and consequent strike variation from WSW-ENE to NW-SE, from west to east, respectively (Fig. 3; Tranos and Mountrakis, 2004; Mountrakis *et al.*, 2006). Four segments are suggested for the whole shear zone, but the length of each proposed segment is probably not sufficient to produce at least moderate events; additionally the geometric characteristics of the segment boundaries are not well defined. Accordingly, no specific ISSs have been included in GreDaSS. The western E-W trending sector (*ca.* 20 km) shows the most prominent fault trace, while a subtle scarp in Pleistocene deposits continues SE-wards possibly making the total length more than 30 km. Morphotectonic evidence of recent activity is not homogeneous along strike and it is mainly represented by a 7 m-high fault scarps affecting Late Pleistocene deposits in the central sector (Tranos and Mountrakis, 2004). No historical nor instrumental earthquakes are associated with this fault zone, but this crustal scale tectonic structure is certainly capable of generating moderate to strong seismic events as far as it is optimally oriented with respect to the present-day stress field and it fills a structural gap between the Drama CSS, to the east, and the Belles CSS, to the west, thus contributing to accommodate the regional N-S lithospheric stretching affecting the Southern Aegean.

3.5. Belles CSS (Petritsi and Kastanoussa ISSs)

Belles CSS is an almost 60 km-long fault zone bordering an impressive linear mountain front and being characterized by thick multi-generation alluvial fans accummulated in the hanging-wall block (Fig. 3; Psilovikos and Papaphilippou, 1990; Mariolakos *et al.*, 2004; Pavlides *et al.*, 2004a). The whole Mount Kerkini (commonly referred to as Belles), which represents the border between Greece and Bulgaria, has been considered a recent tectonic horst by Psilovikos (1984). On the basis of morphotectonic mapping and morphometric analyses, the fault zone has been active during Quaternary and especially the Holocene, while the observed striations are mechanically compatible with the present-day extensional stress field (Pavlides *et al.*, 2004a).

Mountrakis *et al.* (2006) separated the fault zone into two major segments that were approximately adopted in the database: *Petritsi* and *Kastanoussa* ISSs, east and west, respectively.

Both segments show similar lengths (25-26 km each) and a slight right-stepping geometrical relationship. Lateral variations in the degree of activity are debated. For example, based on several geomorphic features (well-developed fault scarps with accelerated erosion, deposition of younger generations of alluvial fans upon older fan heads close to the fault zone, more extensive fan deposits, slightly entrenched torrents and much higher elevations of the fan heads), Psilovikos and Papaphilippou (1990) suggest a higher activity on the western sector, while based on the deflection of the Strymon River (Pavlides *et al.*, 2004; Mariolakos *et al.*, 2004) and a low value of the mountain front sinuosity index, the eastern sector is suggested to be more active.

No major historical earthquakes are reported in the catalogues. It is noteworthy that immediately N-NW of the Doirani Lake an instrumentally recorded seismic sequence (May-October 2009) with an M_w = 5.2 as strongest event (Kiratzi, 2010) suggests the occurrence of an antithetic NNE-dipping normal fault thus implying that the Belles CSS comes to an end close to the Greece-FYROM border.

According to empirical relationships, the mean displacement for each segment is 0.60 m and the maximum expected magnitudes are 6.7 and 6.8 for the Kastanoussa and Petritsi ISSs, respectively. Due to the limited separation between the two segments, their breaching (worst case scenario) is highly possible and could produce a larger event (*ca.* 7.0).

4. The Chalkidiki fault system

The active faults affecting the Chalkidiki peninsula (Fig. 4) are grouped separately from the northern E-W trending fault belt due to their slightly different mean orientation, which is ESE-WNW, but especially because they form two fault sets consisting of shortly spaced subparallel synthetic highly-dipping normal faults possibly linked at depth by a low-angle shear zone (Sboras and Caputo, 2010). The eastern fault set is mainly SSW-dipping, while the western one is NNE-dipping. Both fault sets are delimited by an antithetic structure, south and north, respectively, also included in the database. The eastern set is formed by the Stratoni-Varvara, Gomati and Siggitikos Gulf CSSs and the Vourvourou ISS, while the western set of faults by the Sochos-Mavrouda, Mygdonia, Asvestochori, Pylaea and Anthemoundas CSSs.

In the area, during historical and recent times occurred three major earthquakes (Fig. 4; 1932 Ierissos; 1978 Thessaloniki; 1933, May 11, Thessaloniki). For the former two events the causative fault is well established, while the latter has been tentatively associated with the Gomati CSS. All of them will be discussed in the following paragraphs. However, prior to the 20th century several moderate events are listed in the historical catalogues (Papazachos and Papazachou, 1997; Ambraseys, 2009). For example, in the western Mygdonia Basin are reported the following events (Papazachos and Papazachou, 1997): i) in 700 AD of M_e = 6.5, which is characterized as a 'spurious' event according to Ambraseys (2009), ii) in July, 1420 (M_e = 6.0), a quite destructive event for the city of Thessaloniki (Ambraseys, 2009), iii) on March 26, 1430 (M_e = 6.0), an event that caused some damage to the city walls (Ambraseys, 2009). At the eastern part of the basin only one event of magnitude 6.4 is reported in the catalogue of Papazachos and Papazachou (1997) in the year 677 AD, but considered 'spurious' by Ambraseys (2009). The available historical information for all these events however is not sufficient to accurately locate the epicenter, to estimate the real magnitude and therefore to associate them to any specific causative fault.

4.1. Stratoni-Varvara CSS (Varvara, West Stratoni and East Stratoni ISSs)

The Stratoni-Varvara CSS is a S-SW dipping fault zone affecting the eastern coast of Chalkidiki peninsula, bordering to the south the Stratoniki Mount and largely continuing offshore (Fig. 4). The CSS was reactivated on September 26, 1932 by a strong linear morphogenic event with magnitude 7.0 (Papazachos and Papazachou, 1997) or 6.9 (Ambraseys and Jackson, 1998). Co-seismic effects were plenty enough to confirm that the Stratoni-Varvara CSS was the causative tectonic structure. Ground ruptures (Floras, 1933), many of which coincided with the mapped geological fault, were preserved even decades after (Pavlides and Tranos, 1991). A coastal subsidence of 1.6 m (reported by Floras, 1933, from Pavlides and Tranos, 1991) and a downthrow of approximately 1.8 m across the fault scarp can be inferred from photographic archives (*e.g.* Georgalas and Galanopoulos, 1953).

Although the co-seismic ruptures and the strong recorded magnitude suggest that the 1932 event

ruptured the largest portion of the fault surface, morphotectonic investigations indicate that the Stratoni-Varvara CSS is segmented in three parts showing independent seismotectonic evolutions (Chatzipetros *et al.*, 2005; Michailidou *et al.*, 2005; Pavlides *et al.*, 2010). The *Varvara* ISS is the westernmost segment, 6.5 km-long and probably consisting of several parallel sliding planes with a general WNW-ESE strike. It forms an angular barrier with the adjacent *West Stratoni* ISS (10 km). The last segment (*East Stratoni* ISS) mainly runs offshore and clearly controls the E-W trending coastline up to the Eleftheronesos Island (10 km). Based on the observed maximum displacement documented near Stratoni and caused by the 1932, Ierissos earthquake (Floras, 1933; Georgalas and Galanopoulos, 1953; Pavlides and Caputo, 2004), the CSS probably continues further kilometers eastwards thus producing a total length of *ca.* 37 km. Field measurements along the fault trace (Pavlides and Tranos, 1991) and the microseismicity distribution at depth (Galanis *et al.*, 2004) indicate a steeply dipping fault plane. On the basis of the available seismological information, the maximum depth of the structure is likely 16-18 km. Estimated values of mean co-seismic displacement for the three segments range between 0.33 to 0.43 m, while for the whole CSS could be as high as 1.4 m. The 1932 event (M = 6.9-7.0) likely corresponds to the worst case scenario and represents the maximum expected magnitude for this CSS.

4.2. Gomati CSS

Roughly parallel to and synthetic with the Stratoni-Varvara CSS, is the Gomati fault zone (Fig. 4). Available information is generally scant and uncertainty for many parameters is consequently high. Mainly based on morphotectonic investigations and meso-structural analyses (Pavlides and Kilias, 1987; Michailidou, 2005; Chatzipetros *et al.*, 2005; Michailidou *et al.*, 2005), this tectonic structure is characterized by a major linear escarpment striking 110°-135° and dipping ~65° toward SSW. Field observations of slickenlines indicate a rake of 300°-325° (Pavlides and Kilias, 1987). The 3-D relocation of a set of earthquakes in the Chalkidiki peninsula (Galanis *et al.*, 2004), indicate seismogenic depths up to 16-17 km for this zone, while a relocated seismic cluster suggests the eastwards continuation of the fault zone offshore and north of the Island Amoliani (Galanis *et al.*, 2004), thus defining a total length of *ca.* 30 km.

In concomitance with the 1932 Ierissos seismic crisis, a large number of strong foreshocks and aftershocks were also recorded in the broader area (Papazachos and Papazachou, 1997). It is usually assumed that the magnitude M = 6.3 event which occurred on May 11, 1933 belongs to this seismic sequence and represents an aftershock of the Ierissos mainshock. However, based on a recent relocation of this event several kilometres southwards (Papazachos *et al.*, 2009) and taking into account the long time period elapsed since the main shock, we tentatively associate the 1933 event with the Gomati CSS which was partly reactivated due to a triggering effect. The maximum expected magnitude for the Gomati CSS obtained from empirical relationships is 6.8 (Pavlides and Caputo, 2004).

4.3. Siggitikos Gulf CSS

Also the Siggitikos Gulf CSS belongs to the same system of SSW-dipping normal faults affecting the eastern sector of the Chalkidiki peninsula (Fig. 4). However, its total length is double than the Gomati CSS and also greater than the Stratoni-Varvara CSS. The onshore part of this tectonic structure can be morphotectonically mapped (Pavlides and Kilias, 1987) showing an oblique-slip kinematics with normal and left-lateral components. On the basis of detailed bathymetric maps the CSS probably continues offshore running south of the Island Amoliani and generating the E-W trending coastal escarpment in the Athos Peninsula. It possibly continues eastwards across the Athos Peninsula, though specific field investigations have been not carried out. Information is also scant as concerns possible segmentation. Assuming the worst case scenario, a maximum expected magnitude of 7.1 can be estimated.

4.4. Vourvourou ISS

The southernmost structure of the east Chalkidiki peninsula fault set is represented by the Vourvourou ISS (Fig. 4; Tranos, 1998; Mountrakis *et al.*, 2006); also referred to as Sithonia Fault by Goldsworthy *et al.* (2002). Although the strike of the fault is similar (ESE-WNW), this ISS is northdipping, that is antithetic with respect to the Siggitikos, Gomati and Stratoni-Varvara CSSs. Morphotectonic investigation and meso-structural analyses across the Sithonia peninsula (Tranos, 1998) document a Quaternary activity for *ca.* 15 km and the occurrence of two minor segments, but too small for generating moderate events. The assumed total length of the seismogenic structure is 27 km. The estimated slip-per-event of the Vourvourou ISS is 0.6 m, while the maximum expected magnitude is 6.8 based on empirical relationships (Pavlides and Caputo, 2004).

4.5. Sochos-Mavrouda CSS (Sochos and Mavrouda ISSs)

As above mentioned, another important fault set consisting of several subparallel and largely overlapping CSSs affects the central-western sector of the Chalkidiki peninsula (Fig. 4). The northernmost structure, north of the Mygdonia Basin, is the Sochos-Mavrouda CSS, which is antithetic with respect to the other ones, being the only one characterized by a south-dipping setting. The Sochos-Mavrouda fault zone is *ca.* 41 km-long and forms small intra-mountain basins (Maravelakis, 1936). It is considered active based on the occurrence of triangular facets in the footwall and thick Quaternary scree and fan sediments accummulated in the hanging-wall (Mountrakis *et al.*, 1996a; 2006). At least two *ca.* 9 km-long segments have been recognized: *Sochos* and *Mavrouda* ISSs (Goldsworthy *et al.*, 2002; Mountrakis *et al.*, 2006). The segment boundary is represented by a marked gap with a right-stepping underlapping geometry, therefore making unlikely a continuous rupture process in case of reactivation. The two segments are singularly capable of producing a maximum magnitude of 6.3 (Pavlides and Caputo, 2004), while in case of a complete reactivation of the western sector (~29 km) the maximum expected magnitude is 6.8. The westernmost section of the fault zone is

characterized by microseismic activity (Galanis *et al.*, 2004; Paradisopoulou *et al.*, 2004). According to 3-D re-location of the local seismicity (Galanis *et al.*, 2004) the seismogenic layer thickness is approximately 13-15 km. The Sochos-Mavrouda CSS is a possible candidate for the 1902, July 5, Assiros earthquake (M = 6.5; Papazachos and Papazachou, 1997), though we have tentatively attributed this event to the Langadhas ISS (see Mygdonia CSS) according to a critical revision of the available historical information.

4.6. Mygdonia CSS (Apollonia, Gerakarou and Langadhas ISSs)

South of the Sochos-Mavrouda CSS, but with an antithetic north-dipping setting is the major Mygdonia CSS bordering to the south the homonymous basin for a total length of *ca.* 67 km (Fig. 4). The fault trace follows the mountain front and shows important strike variations due to the curved morphology due to segmentation. The fault zone was first mapped by Kockel and Mollat (1977), but most structural and morphotectonic investigations were carried out after the 1978, June 20, Thessaloniki earthquake (M_w = 6.5), which re-activated the central segment of the Mygdonia CSS (Mercier *et al.*, 1979; 1983; Mountrakis *et al.*, 1996a; Tranos *et al.*, 2003). Three main segments can be recognised (from east to west): *Apollonia*, *Gerakarou* and *Langadhas* ISSs.

The eastern *Apollonia* Fault segment, has sculptured a prominent linear morphology which is interrupted by the alluvial fan of the Megalo Rema. A conservative value for the fault length is 20 km and the segment boundary with the Gerakarou Fault is marked by a change in strike. Microearthquake surveys document a dip-slip kinematics on the Apollonia ISS (Hatzfeld *et al.*, 1986/87), while the 3-D relocation of the seismicity shows activity down to a depth of 18 km and delineates a steeply dipping fault plane (Galanis *et al.*, 2004). Based on empirical relationships, the potential amount of slip-per-event is 0.65 m, while 6.5 is the maximum expected magnitude.

The central sector of the CSS is represented by the *Gerakarou* ISS which is the causative fault of the June 20, 1978 earthquake. This earthquake has been thoroughly studied due to its location very close to Thessaloniki city. Extended co-seismic ground ruptures were produced that splayed out in the Mygdonia Basin (Mercier *et al.*, 1979; 1983; Papazachos *et al.*, 1979; Soufleris and Stewart, 1981; Mountrakis *et al.*, 1996a). The most significant ones occurred along the southern margin of the basin, coinciding with the principal N-dipping fault escarpment. Two other groups of aligned ruptures were observed near to the centre of the basin, between the lakes of Koronia and Volvi. In particular, the northernmost one strikes NW-SE, shows a south-dipping normal displacement and it probably represents a secondary accommodation structure. Seismotectonic parameters are well constrained on the basis of focal mechanisms, source parameters of the mainshock and the aftershock distribution (Kulhánek and Meyer, 1979; Papazachos *et al.*, 1979; Barker and Langston, 1981; Carver and Bollinger, 1981; Soufleris and Stewart, 1981; Soufleris *et al.*, 1982; Soufleris and King, 1983; Dziewonski *et al.*, 1987; Vannucci and Gasperini; 2003; 2004; Roumelioti *et al.*, 2007) as well as several morphotectonic investigations and meso-structural analyses (Mercier *et al.*, 1979; 1983;

Mountrakis *et al.*, 1996a; Tranos *et al.*, 2003). The ruptured fault plane strikes almost E-W, dips northwards with shallow to moderate angle and is characterized by an almost pure dip-slip normal motion associated with a N-S direction of crustal extension. Microearthquake surveys suggest a listric fault geometry with a knick-point at 8 km depth and a seismogenic layer thickness ranging between 14 and 16 km (Hatzfeld *et al.*, 1986/87; Tranos *et al.*, 2003; Paradisopoulou *et al.*, 2006), which is shallower with respect to the eastern segment. Stiros and Drakos (2000) suggest blind faulting during the 1978 event considering the observed surface ruptures only secondary effects. In contrast, palaeoseismological trenches confirm the occurrence of repeated linear morphogenic events before the 1978 (Cheng *et al.*, 1994; Chatzipetros, 1998; Chatzipetros *et al.*, 2004) with a mean slip-per-event of 6.5-16 cm, a slip-rate of 0.06-0.7 mm/a and a recurrence interval ranging between 1000 and 1500 years. Slip-per-event at the fault-scale is probably underestimated considering the magnitude of the 1978 earthquake; based on seismic waveforms joint inversion and levelling data a value of 0.6 m is preferred (Roumelioti *et al.*, 2007).

The westernmost segment (*Langadhas* ISS) exhibits a sharp mountain front with a NW-SE direction. Although this structure has been clearly inherited from previous tectonic events (both alpine thrusting and Miocene-Pliocene NE-SW extension) and it is not ideally oriented with the present-day regional stress field, it shows evidences of recent reactivations with an oblique-slip kinematics (Mercier *et al.*, 1979; 1983) as also supported by morphometric parameters (very low mountain-front sinuosity index). In contrast, Tranos *et al.* (2003) suggest that this portion of the Mygdonia CSS has been abandoned and that activity has migrated southern towards the Asvestochori CSS (see §4.7). Microseismic activity (Galanis *et al.*, 2004; Paradisopoulou *et al.*, 2006) indicate a maximum depth of 14-16 km. The estimated mean displacement is 0.51 m and the maximum expected magnitude is 6.6 (Pavlides and Caputo, 2004). As above mentioned and according to the available historical information, the 1902, July 5, Assiros earthquake (M = 6.5; Papazachos and Papazachou, 1997), has been tentatively attributed to the Langadhas ISS.

4.7. Asvestochori CSS

This fault zone lies very near to the urban area of Thessaloniki; it runs parallel to, and is synthetic with, the western segment of the Mygdonia CSS (Fig. 4). The fault is reported in several morphotectonic and geological maps (Mountrakis *et al.*, 1996a; 1996b; Tranos *et al.* 2003; Zervopoulou, 2004). According to Mercier *et al.* (1983), the Asvestochori Fault was partially reactivated during the 1978 Thessaloniki earthquake. According to Tranos *et al.* (2003), the recent growth of this structure has progressively de-activated the Langadhas ISS and is going to produce a direct linkage with the central sector of the Mygdonia CSS. Information for the deeper parts of the fault is provided by microearthquake investigations (Paradisopoulou *et al.*, 2006) and geological considerations (Tranos *et al.*, 2003), both implying the existence of a listric geometry with a dip varying from 80° at the surface to 35° at depth. The maximum seismogenic depth is constrained to 15-

16 km based on microseismic distribution (Galanis *et al.*, 2004; Paradisopoulou *et al.*, 2004).

4.8. Pylaea CSS

This seismogenic structure is important because directly crosses the urban area of Thessaloniki and its gulf (Fig. 4). The fault trace has been mapped by Mountrakis *et al.* (1996b), Tranos *et al.* (2003), Zervopoulou (2004) and Valkaniotis *et al.* (2005), providing constraints on its location, surface geometry and strike. Considering that this tectonic structure belongs to the broader normal fault set that affects the central-western Chalkidiki peninsula and that it possibly represents an upwards splay of a deeper low-angle normal detachment (Tranos *et al.*, 2003), the other principal seismotectonic parameters have been inferred accordingly. The extension of this fault towards the West to the city of Thessaloniki has been mapped as Voulgari Street Fault by Zervopoulou (2009).

4.9. Anthemountas CSS (Souroti and Angelochori ISSs)

The Anthemountas Fault (Mountrakis *et al.,* 1993b) is also an important structure for the Thessaloniki urban area because it bounds the southern side of the gulf and has been mapped for a total length of at least 40 km (Fig. 4). It possibly extends more to the west, offshore in the Thermaikos Gulf. According to Tranos *et al.* (2003) this structure represents the southernmost north-dipping high-angle splay fault joining at depth a regional-scale low-angle extensional shear zone kinematically linked to the Pylaea, Asvestochori and Mygdonia CSSs. The fault has been tentatively separated into two segments according to morphotectonic criteria (Zervopoulou, 2004; Zervopoulou and Pavlides, 2005; Zervopoulou *et al.*, 2007): *Souroti* and *Angelochori* ISSs, east and west, respectively, both characterized by a length of ~17 km.

In 1759 an important seismic sequence affected the city of Thessaloniki (Papazachos and Papazachou, 1997; Ambraseys, 2009). The date of the major shock is debated. Papazachos and Papazachou (1997) suggest the 22nd of June, while Ambraseys (2009) states that during June 22 two 'violent' shocks indeed occurred, but the destructive event took place on the 3rd of July. The macroseismic magnitude was 6.5 and the aftershock sequence was intensive (Papazachos and Papazachou, 1997). According to the tentative location of the macroseismic epicenter the causative fault could be the Angelochori ISS. In 1677 another earthquake with estimated macroseismic magnitude 6.2 caused damages in several villages east of Thessaloniki (Papazachos and Papazachou, 1997; Ambraseys, 2009). Based on the suggested macroseismic epicenter and considering that *ca.* 80 years later the western segment was probably re-activated (1759 event), the 1677 is tentatively associated with the Souroti ISS (eastern segment). It is noteworthy that aseismic creep has been observed along the Angelochori Fault (Zervopoulou *et al.*, 2007). Assuming an independent rupture of the two segments, the estimated mean displacement is 0.59 m and the maximum expected magnitude is 6.5 (Valkaniotis *et al.*, 2005), which become 1.35 m and M = 6.9 in the worst case scenario (*i.e.* entire fault rupture).

5. The 'anti-Hellenides' fault system

West of the Vardar Valley, in Western Macedonia and Epirus, the orographic and morphological first-order texture of the region is characterized by the NW-SE trending Hellenic fold-and-thrust belt which has generated elongated mountain chains and interposed valleys (Fig. 5). In this sector of northern Greece, all major active faults that have been recognized at present and included in GreDaSS are oriented NE-SW, therefore showing a typical 'anti-Hellenides' (anti-orogenic) setting. It is worth noting that stress trajectories reconstructed for this region show a NNW to NW orientation of the σ_3 stress axis (*e.g.* Mercier *et al.*, 1989; Jenny *et al.*, 2004).

Within this fault system GreDaSS includes several 'isolated' CSSs and ISSs, like the North Almopia, South Almopia, Goumenissa, Aliakmonas, Konitsa and Petoussi. In contrast, the Ptolemaida Basin is affected by a group of sub-parallel, synthetic and antithetic, seismogenic structures which are possibly linked at depth by a low-angle shear zone, showing a seismotectonic setting similar to that described in the Chalkidiki peninsula (Sboras and Caputo, 2010).

5.1. North Almopia CSS (Pozar, Promachi and Aetochori ISSs)

The North Almopia fault zone has a total length of *ca.* 38 km, bounding the northern margin of the Almopia Basin and a smaller adjacent basin to the northeast (Fig. 5; Pavlides *et al.*, 1990; Goldsworthy *et al.*, 2002; Vougioukalakis, 2002; Mountrakis *et al.*, 2006). The development of the Almopia Basin took place during Pliocene and was accompanied by significant volcanic activity (Mercier, 1981). Vougioukalakis (2002) however, suggests that the subsidence of the basin occurred only after the end of the volcanism (1.8 Ma), *i.e.* during the Quaternary.

The zone can be divided into three major segments (Goldsworthy *et al.*, 2002; Mountrakis *et al.*, 2006): *Pozar*, *Promachi* and *Aetochori* ISSs (from east to west), forming an overall left-stepping geometry. Meso-structural analyses provide important geometric and kinematic information (Mercier *et al.*, 1989; Pavlides *et al.*, 1990) indicating that two slightly different extensional tectonic phases took place from Middle Pleistocene to Present, with the most recent stress field characterized by a NNW-SSE direction of extension. Using electrical resistivity tomographies, borehole data and field observations, Vougioukalakis (2002) carried out a 3-D structural reconstruction of the basin and estimated for the central sector vertical and horizontal extension rates of 0.92 mm/a and 0.36 mm/a, respectively. Slip-per-event and maximum expected magnitude for the three segments are (from east to west) 0.36, 0.47 and 0.30 m and 6.1, 6.3 and 5.9, respectively. However, the worst case scenario considers the joint reactivation of the two western segments (Pozar and Promachi ISSs) with a maximum expected magnitude of 6.9 (Pavlides and Caputo, 2004), given that the Aetochori ISS shows a great overstep and underlap which should likely act as a strong barrier.

5.2. Goumenissa ISS

Information for this seismogenic structure mainly derives from the December 21, 1990 (Ms = 6.0) Goumenissa earthquake (Panagiotopoulos *et al.*, 1993). The fault evidence at the surface is somehow questionable; the fault is possibly blind due to the fact that the estimated focal depth is *ca.* 16 km (Fig. 5). In any case the event did not produce any observable ground ruptures. The aftershock spatial distribution indicates a length of at least 15 km, while the analysis of the main shock suggests a mean displacement of 0.45 m. The focal mechanisms show a SE-dipping, NE-SW trending dip-slip normal fault (Dziewonski *et al.*, 1991; Panagiotopoulos *et al.*, 1993; Baker *et al.*, 1997; Vannucci and Gasperini, 2003; 2004).

In the vicinity of the Goumenissa ISS on October 1395 occurred the so-called Edessa earthquake (Ambraseys, 1999; 2009) with a possible magnitude of 6.7 (Papazachos and Papazachou, 1997). However, the tentative location of the macroseismic epicenter is similarly close to the South Almopia CSS and not very far from the North Almopia CSS (see §5.1). Accordingly, the state-of-knowledge does not allow associating this strong earthquake with any recognized structure.

5.3. South Almopia CSS

The South Almopia CSS is 20 km-long and dips towards the south, showing a marked arcuate fault trace (Fig. 5). Information about the fault derives from morphotectonic investigations (Pavlides, 1998), which document ENE-WSW-striking, dip-slip normal faults affecting the pyroclastic sediments formed 4.8 Ma ago. The mesostructural analysis of these deposits reveals a NNW-SSE direction of the σ_3 axis. The measured dip-angle of the faults is high. The structure is considered active also due to its ideal orientation with respect to the regional stress field. Assuming a complete reactivation of the whole fault zone, the maximum expected magnitude is 6.7.

5.4. Amyndeo CSS (Nymfeo and Petron ISSs)

As mentioned above, the Ptolemaida Basin is a tectonically controlled area characterized by alternating sub-parallel ridges and basins, all elongated in a NE-SW direction (Pavlides, 1985) and associated with subparallel fault zones possibly linked at depth by a low-angle SE-dipping shear zone (Fig. 5). Several major fault zones, controlling large morphological structures, and smaller individual ones, but not less significant, have been recognised and studied (Pavlides, 1985; Pavlides and Mountrakis, 1987; Doutsos and Koukouvelas, 1998; Goldsworthy *et al.*, 2002). Field measurements of all the active tectonic structures in the Ptolemaida Basin indicate a (N)NW-(S)SE direction of the slip vector (Pavlides, 1985; Pavlides and Mountrakis, 1987; Doutsos and Koukouvelas, 1998). Although the morphotectonic features of the area indicate intensive and recent activity, neither historical nor instrumental significant seismic activity is recorded. The seismogenic layer thickness of *ca.* 11 km is inferred from seismotectonic considerations (Pavlides and Simeakis, 1987/88).

The northernmost structure is the Amyndeo CSS showing clear geological and morphological

evidence of recent activity (Pavlides, 1985; Pavlides and Mountrakis, 1987; Doutsos and Koukouvelas, 1998; Goldsworthy *et al.*, 2002). The Amyndeo fault zone borders and tectonically controls the mountain front along a SW-trending ridge that separates the Ptolemaida Basin from the Florina Basin to the north and connects the two mountains of Voras, to the east, and Vernon, to the west. All along its almost 40 km of total length, it has produced a discrete morphological slope as a result of a major dip-slip normal motion with a slight right-lateral strike-slip component as documented by slickenlines (Pavlides, 1985). However, the fault zone is not entirely uniform. West of Petron village, the relief locally becomes subdued, while a slight change of the mountain front orientation is observed. Accordingly, the fault zone is divided into two segments: *Petron* and *Nymfaeo* ISSs, NE and SW respectively.

The *Petron* ISS is a *ca.* 9 km-long structure that controls the local depression where the Petron Lake is located. The fault has shaped a linear and steep coastline on Mesozoic limestones, characterized by evident slickensides affecting scree deposits and cataclastic breccias (Pavlides, 1985). The fault trace continues northeastwards for 2-3 km forming a small narrow valley. Towards the southwest the fault cuts through Neogene sediments (upper Miocene-lower Pliocene), while NNE-trending secondary structures affect also Pleistocene deposits. The southwestern fault-tip is covered by Pliocene-Pleistocene sediments suggesting that the Petron-Nymfaeo segment boundary likely corresponds to a permanent barrier.

The *Nymfaeo* ISS is a larger (13 km-long) NE-SW trending structure showing angular segment boundary geometry. Near to its northeastern tip, the fault affects and downthrows Pliocene sediments (Pavlides, 1985). Towards the SW, a mojor escarpment possibly documents a cumulative displacement up to 700-800 m. The fault has been also detected by Vertical Electrical Soundings (VES) and boreholes (Atzemoglou *et al.*, 2003).

The two ISSs are capable of producing 6.0 and 6.2 earthquakes, respectively, with a mean coseismic displacement of 0.38 m and 0.48 m. However, both ISSs could possibly extend further NE and SW, respectively (worst case scenario), therefore the maximum expected magnitudes could be as high as 6.6-6.7.

5.5. Chimatidis ISS

Parallel and antithetic to the Nymfaeo ISS a 12 km-long active tectonic structure lies along the southern shore of Chimaditis Lake (Fig. 5; Pavlides, 1985; Pavlides and Mountrakis, 1987). The NW-dipping dip-slip normal Chimaditis ISS has generated a low elongated terrace on its footwall consisting of uplifted Neogene, Pleistocene and Holocene deposits (Pavlides, 1985). This structure probably joins the Nymfaeo ISS at depth constraining its maximum depth to *ca.* 7.5 km. Accordingly, the maximum expected magnitude is probably < 6.0.

5.6. Ptolemaida CSS (Vegoritida and Vegora ISSs)

Parallel to and synthetic with the central-northern sector of the Amyndeo CSS, there is the 25 km-long Ptolemaida CSS (Fig. 5). The fault zone and shows clear morphotectonic evidences of recent activity and consists of two segments: *Vegoritida* and *Vegora* ISSs, NE and SW respectively.

The *ca.* 10 km-long, (N)NE-trending *Vegoritida* ISS shows an impressive morphology with a high limestone cliff, and bordering the homonymous lake. A minimum cumulative downthrow of 500 m is morphologically inferred (Pavlides, 1985), while high-resolution Boomer profiles carried out in the lake, suggest a vertical stratigraphic displacement of about 600-700 m (Sakellariou *et al.*, 2001). Mesostructural analyses document a recent NNW-SSE trending direction of stretching (Pavlides, 1985; Pavlides and Mountrakis, 1987; Doutsos and Koukouvelas, 1998; Mountrakis *et al.*, 2006).

The *Vegora* ISS continues for at least 12 km southwestwards forming an arcuate escarpment (Pavlides, 1985; Pavlides and Mountrakis, 1987; Doutsos and Koukouvelas, 1998). The absence of limestones in the footwall of this fault causes a more subtle morphology. Few scattered limestone outcropping scarps, nevertheless, bear striations that indicate a roughly dip-slip normal kinematics associated with a NW-SE direction of extension (Pavlides, 1985). Neogene and Quaternary sediments are affected by the fault. The high-resolution Boomer profiles of the lake bottom suggest an offshore continuation of the fault (Sakellariou *et al.*, 2001). As a result, the fault overlaps the Vegoritida ISS, probably reaching a total length of more than 14 km.

Each fault segment is capable of producing an earthquake of 6.0 and 6.2 with a mean co-seismic displacement of 0.40 m and 0.49 m (Vegoritida and Vegora ISS respectively). However, a rupture of the entire fault zone is a possible (worst case) scenario, given that the segment boundary does not seem strong enough to prevent it. In this case, the maximum estimated magnitude would be 6.7.

5.7. Perdika ISS

Sub-parallel to and synthetic with the Chimatidis Fault (see §5.5) is the Perdika ISS, which lies 6 km southwards (Fig. 5; Pavlides, 1985; Pavlides and Mountrakis, 1987; Goldsworthy *et al.*, 2002; Mountrakis *et al.*, 2006). The Perdika ISS is a 12 km-long structure that borders the northern hillside of the Bordeaux Heights, separating the Pliocene(?) sediments outcropping in the footwall from the Quaternary deposits of the plain. For similarity with the other structures of the broader Ptolemaida Basin and according to the regional stress field, the kinematics of the Perdika Fault is basically dip-slip normal. A possible reactivation of the fault can produce an earthquake with maximum expected magnitude of 6.0.

5.8. Komanos CSS (Mesovouni and Proastio ISSs)

The (N)NE-(S)SW trending and NW-dipping Komanos CSS bounds the southeasternmost margin of the Ptolemaida Basin (Fig. 5; Pavlides, 1985; Pavlides and Mountrakis, 1987; Mountrakis *et al.*, 2006). Two major segments have been recognized: *Mesovouni* and *Proastio* ISSs, NE and SW

respectively (Mountrakis *et al.*, 2006). The fault zone has a total length of *ca.* 36 km, though morphological evidence in the central sector is poor and introduce some uncertainty in the location of the segment boundary. Both segments indicate a steep NW-dipping angle.

The *Mesovouni* ISS runs along the northwestern front of the Mount Vermion for at least 17 km (Pavlides, 1985; Pavlides and Mountrakis, 1987; Doutsos and Koukouvelas, 1998; Mountrakis *et al.*, 2006), showing a low value of the mountain front sinuosity index. Quaternary deposits have been mainly accumulated within a secondary accommodation structure (a 1.5 km-wide symmetric graben) thus suggesting the recent activity of this fault (Pavlides, 1985; Pavlides and Mountrakis, 1987; Mountrakis *et al.*, 2006). The measured cumulative displacements in Pliocene lignite deposits, deriving from borehole data, range from 20-40 m up to 70 m (Pavlides, 1985). On July 9, 1984 a moderate earthquake (M_w = 5.2) occurred between the Mesovouni and the Peraea ISSs (see §5.9; Pavlides and Simeakis, 1987/88; Dziewonski *et al.*, 1985; Anderson and Jackson, 1987). The obtained focal mechanisms are in agreement with the local tectonic setting and specifically with the seismotectonic features of the Mesovouni Fault (Dziewonski *et al.*, 1985; Anderson and Jackson, 1987).

The *Proastio* ISS lies on the northern borders of the lignite mines (Pavlides, 1985; Pavlides and Mountrakis, 1987; Doutsos and Koukouvelas, 1998; Mountrakis *et al.*, 2006). It is expressed by a group of parallel minor fault scarps affecting Quaternary sediments. Northwards it has been detected by boreholes showing a down-stepping throw of the Pliocene lignite deposits with a cumulative displacement of almost 300-400 m (Pavlides, 1985). Secondary antithetic structures were also observed on the footwall forming a minor tectonic horst (Pavlides, 1985; Diamantopoulos, 2006). The fault zone extends for *ca.* 10 km. Kinematic indicators document an almost pure dip-slip normal motion (Pavlides, 1985; Pavlides and Mountrakis, 1987) and a NW-SE direction of extension.

Individual reactivation of each segment can produce events of 6.2 and 6.0 (maximum expected magnitudes; Mesovouni and Proastio ISSs, respectively). Their corresponding co-seismic mean displacement is estimated to 0.52 and 0.37 m. Since the boundary between the two segments is not clearly observed and especially its nature (*i.e.* strong or soft boundary), the possible rupture of the entire fault zone cannot be excluded a priori. In this case (worst case scenario), the maximum expected magnitude would be 6.6.

5.9. Peraea ISS

The Peraea ISS (Fig. 5) is an active structure close to but antithetic with the Komanos CSS (see §5.8) and at the same time synthetic to the Ptolemaida CSS (see §5.6; Pavlides, 1985; Pavlides and Mountrakis, 1987; Goldsworthy and Jackson, 2000; 2001; Mountrakis *et al.*, 2006). The SE-dipping fault is marked by a discontinuous escarpment that extends for a total length of *ca.* 14 km. Impressive slickensides and free faces put in contact the Mesozoic substratum with Holocene deposits (Pavlides, 1985; Goldsworthy and Jackson, 2000; 2001). The estimated mean co-seismic displacement of the

fault is 0.43 m and can produce an earthquake of maximum expected magnitude 6.1.

5.10. Aliakmonas CSS (Palaeochori, Rymnio, Servia and Chromio ISSs)

Aliakmonas fault zone is a NE-SW-trending, NW-dipping major tectonic structure controlling a long reach of the homonymous river (Fig. 5). The total length of the CSS is 64 km. Geological and morphotectonic investigations suggest the occurrence of three major segments: *Palaeochori*, *Rymnio* and *Servia* (from SW to NE; Pavlides *et al.*, 1995; Chatzipetros, 1998; Doutsos and Koukouvelas, 1998; Mountrakis *et al.*, 1998; Meyer *et al.*, 1996; 1998). The aftershock spatial distribution of an event that occurred during 1995 (see below the Palaeochori ISS) (Hatzfeld *et al.*, 1997; 1998) documents a maximum seismogenic depth of 15 km, which possibly becomes gradually shallower from the south-western to the north-eastern part of the fault zone. Moreover, based on morphological evidence, Doutsos and Koukouvelas (1998) suggest a recent westward migration of the tectonic activity. The penultimate strong event in the area has been reported by Stiros (1998) and Ambraseys (1999) and is dated at *ca.* 1700 (possibly 1695), based on historical data.

The *Palaeochori* ISSs is marked by a *ca.* 21 km-long discontinuous escarpment that fades away towards SW (Pavlides *et al.*, 1995; Doutsos and Koukouvelas, 1998; Mountrakis *et al.*, 1998). It was reactivated during the May 15, 1995 Kozani earthquake (M_w = 6.5) producing aligned, but not continuous, co-seismic ground ruptures all along its length. (Pavlides *et al.*, 1995; Mountrakis *et al.*, 1998). Based on nodal planes from focal mechanisms (Papazachos *et al.*, 1998; Dziewonski *et al.*, 1996; Kiratzi and Louvari, 2003; Vannucci and Gasperini, 2003; 2004), earthquake tomographies from the aftershocks (Chiarabba and Selvaggi, 1997), aftershock spatial distributions (Hatzfeld *et al.*, 1997; 1998), stress tensor inversions (Kiratzi, 1999), forward modelling of the source from strong motion waveforms (Suhadolc *et al.*, 2007) and InSAR images analyses (Meyer *et al.*, 1996; 1998; Rigo *et al.*, 2004; Resor *et al.*, 2005) it is possible to constrain several seismotectonic parameters. Based on palaeoseismological investigations a recurrence interval of 10-30 ka is tentatively suggested (Chatzipetros *et al.*, 1998), which is likely overestimated. During the 1995 seismic crisis, the aftershock spatio-temporal distribution revealed the occurrence of a secondary antithetic structure, the *Chromio* ISS (Hatzfeld *et al.*, 1997; 1998), which also produced co-seismic ground ruptures south-dipping and aligned in an E-W direction (Pavlides *et al.*, 1995; Mountrakis *et al.*, 1998) and is considered as an inherited S-dipping right-lateral strike-slip fault reactivated in the new tectonic regime as dip-slip normal fault antithetic to the Palaeochori ISS (Pavlides *et al.*, 1995; Mountrakis *et al.*, 1998; Hatzfeld *et al.*, 1997; 1998).

Northeast of Palaeochori ISS is the *Rymnio* ISS separated by an angular barrier. The fault is marked by a distinct escarpment especially in the northestern sector (Pavlides *et al.*, 1995; Doutsos and Koukouvelas, 1998; Mountrakis *et al.*, 1998). Also the northeastern boundary of the Rymnio segment corresponds to a strong geometric barrier (right-stepping underlapping geometry) (Pavlides *et al.*, 1995; Doutsos and Koukouvelas, 1998; Mountrakis *et al.*, 1998; Meyer *et al.*, 1996; 1998). The

total length is *ca.* 21 km. A partial reactivation of this structure during the 1995 earthquake has been claimed based on some ground ruptures observed near to the Rymnio village. However, their occurrence along the lakeshore likely indicates gravitational phenomena. Morphotectonic investigations (Pavlides *et al.*, 1995; Doutsos and Koukouvelas, 1998; Mountrakis *et al.*, 1998; Meyer *et al.*, 1996; 1998) indicate similar geometry and kinematics with the nearby tectonic structures.

Next to Rymnio Fault is the *Servia* ISS, which represents the most prominent neotectonic structure of the Aliakmonas CSS. The fault is documented by a long, well polished sliding surface on limestones, which bears a set of fresh striations documenting a (N)NW-(S)SE direction of extension (Pavlides *et al.*, 1995; Meyer *et al.*, 1996; 1998; Mountrakis *et al.*, 1998; Gountromihou, 1998; Goldsworthy and Jackson, 2000). There was no sign of reactivation during the 1995 earthquake. The northeastern tip of the fault is not well defined. Based on the asymmetric shape of the along-strike displacement profile, Doutsos and Koukouvelas (1998) suggest a possible linkage between the Servia and Rymnio ISSs. A slip-per-event of 0.52 m is estimated from empirical relationships, while based on geomorphic markers a slip-rate of 1-2 mm/a and a mean recurrence interval of 1-2 ka are suggested (Meyer *et al.*, 1996). A maximum cumulative displacement of 2100 m has been proposed by Doutsos and Koukouvelas (1998) across the fault. On September 26, 1695 an earthquake (M_e = 6.5) struck the area with macroseismic epicentre tentatively located on the hanging-wall of the Rymnio Fault (Papazachos and Papazachou, 1997; Ambraseys, 1999; 2009). However, the lack of details prevents any straightforward correlation with any specific segments of the Aliakmonas CSS.

It is noteworthy that the Aliakmonas CSS continues northeastwards following the valley separating Mount Vermion from the Pieria Mountain chain. For this sector has been tentatively suggested a fourth distinct 25 km-long fault segment (referred to as Polyphytos-Polydendri by Mountrakis *et al.*, 2006), which however does not show definite evidence of recent seismogenic activity. Accordingly, we included this structure in the CSS without defining any specific ISS in GreDaSS.

5.11. Konitsa CSS

The Konitsa CSS is a *ca.* 25 km-long, NW-dipping structure bordering the mountain front of Mount Tymfi (Fig. 5). The best evidence of recent activity is limited to a length of 11 km along the southern margin of the elongated Aoos Basin and corresponds to the Konitsa ISS. In particular, based on several morphotectonic and structural investigations (Doutsos and Koukouvelas, 1998; Doutsos and Kokkalas, 2001; Goldsworthy *et al.*, 2002; Galanakis *et al.*, 2007) the fault is associated with a major escarpment delimited by a linear mountain front. Observations include many fresh slickensides, bearing also corrugations, on the Mesozoic limestone, usually delimiting the Miocene flysch but sometimes also Quaternary deposits. Although Goldsworthy *et al.* (2002) suggest the possible northeastern prolongation of this structure and its connection with the fault system of the Ptolemaida Basin, the Konitsa CSS is mechanically bounded by a roughly perpendicular Neogene thrust which

causes displacement to decrease rapidly eastwards (Doutsos and Koukouvelas, 1998).

On July 26, 1996 a moderate earthquake (M_s = 5.4 according to Papanastassiou (2001) or M_w = 5.1 according to EMMA catalogue (Vannucci and Gasperini, 2003; 2004) occurred near Konitsa town. A couple of weeks later, another moderate but stronger event (M_s = 5.7 according to Papanastassiou (2001) or M_w = 5.3 according to Dziewonski *et al.* (1997)) occurred in the same seismogenic volume. Observed coseismic ruptures (Galanakis *et al.*, 2007) and focal mechanisms (Dziewonski *et al.*, 1997; Vannucci and Gasperini, 2003; 2004) are in agreement with the mesostructural analyses (Doutsos and Koukouvelas, 1998; Doutsos and Kokkalas, 2001; Galanakis *et al.*, 2007) showing a normal dip-slip motion in a NW-stretching field. An average dip-angle of 55° and a maximum depth of *ca.* 11 km are inferred from the aftershock spatial distribution, which also suggest a listric shape at depth (Papanastassiou, 2001). Although the largest magnitude instrumentally recorded during the 1996 sequence was the M_w = 5.3 event, the expected maximum magnitude for the Konitsa ISS is 6.1, with a mean coseismic displacement of 0.40 m. Moreover, if we take into account the total length of the CSS then the maximum expected magnitude could be as high as 6.7.

5.12. Petoussi CSS (Souli and Tomaros ISSs)

The Petoussi CSS is a *ca.* 38 km-long fault zone mainly inherited from the Mesozoic evolution and the Alpine tectonics (Fig. 5; Caputo and Zouros, 1993; Boccaletti *et al.*, 1997). Although the Petoussi CSS has a different strike (~E-W) with respect to the other seismogenic sources included in the Western Macedonia-Epirus fault system, a regional-scale undulation of the orogene makes also this fault zone a typical anti-Hellenic structure. The Petoussi CSS is a sub-vertical fault zone with local changes in dip direction, bearing kinematic indicators that indicate a prominent left-lateral strike-slip motion (Caputo and Zouros, 1993). This geological setting has formed positive and negative flower structures as well as secondary splay faults (Boccaletti *et al.*, 1997). Based on these differences, we divided the fault zone into two major segments, the *Tomaros* and *Souli* ISSs, east and west respectively. The recent activity of the Petoussi CSS is based on morphotectonic investigations and palaeoseismological trenches which document along the Souli Fault at least 3 palaeo-events during the last *ca.* 30 ka BP (Boccaletti *et al.*, 1997), therefore suggesting a recurrence period of several thousand years.

Microearthquake surveys (King *et al.*, 1983; Hatzfeld *et al.*, 1995; Tselentis *et al.*, 2006) document an eastward increase of the seismogenic depth from less than 12 km to more than 15 km and both strike-slip and normal dip-slip focal mechanisms. The estimated mean displacement for the Souli and Tomaros ISSs is 0.49 m and 0.55 m, respectively, while the maximum expected magnitude is 6.2 and 6.3, respectively. In case that the whole Petoussi CSS is re-activated (worst case scenario), the maximum expected event would be 6.9 (Wells and Coppersmith, 1994).

6. The North Aegean offshore fault system

A strong limitation in investigating offshore faults is represented by the complete lack of direct observations; in terms of morphotectonic and geological approaches, only detailed bathymetric maps could serve the scope (*e.g.* Maley and Johnson, 1971; IOC, 1981; Papanikolaou *et al.*, 2002) and seismic reflection investigations (*e.g.* Brooks and Ferentinos, 1980; Mascle and Martin, 1990; Roussos and Lyssimachou, 1991; Papanikolaou *et al.*, 2006). Accordingly, most of the information concerning offshore faults is provided by seismic data like focal mechanisms and microseismic distribution (*e.g.* Dziewonski *et al.*, 1983; 1984; Rocca *et al.*, 1985; Kiratzi, 1991; Taymaz *et al.*, 1991).

The North Aegean Sea is dominated by two regional-scale tectonic structures: the North Aegean Basin (NAB) and the North Aegean Trough (NAT) directly connected and representing the western continuation of the North Anatolian Fault (Fig. 6). The NAB is situated between the Chalkidiki peninsula, Thessalian coast and Sporades Islands. Along strike, it is bordered by two major fault zones which are mainly characterized by a oblique-slip kinematics: *South Chalkidiki offshore* and *North Aegean Basin* CSSs. Minor structures affect the interposed region, but the lack of sufficient data, their likely reduced dimensions (hence limited maximum expected magnitude) and their location far offshore from the Greek coastlines make at present their recognition more problematic and precise seismotectonic definition less urgent. For these reasons they have been not included in this paper.

The other regional-scale tectonic structure (NAT) is represented by a crustal-scale negative flower structure affecting the sea bottom between Callipolis (Gelibolu) peninsula, Limnos and Imbros islands, to the south and Samothraki Island, to the north. In this transtensional shear zone we have recognized two CSSs (*North NAT* and *South NAT*), marking the mechanical-stress transition from the purely transcurrent tectonic regime of the North Anatolian Fault, to the east, and the prevailingly extensional regime towards the west (NAB) (Pavlides *et al.*, 1990; Taymaz *et al.*, 1991; Pavlides and Caputo, 1994; Papanikolaou *et al.*, 2006). Due to this lateral variation, the basin of the NAT progressively widens and deepens westwards (Papanikolaou *et al.*, 2002). For the purposes of this paper we will focus only on the offshore part west of the Callipoli peninsula.

In the North Aegean region other active tectonic structures occur which are synthetic or kinematically associated with those of the NAB and NAT; they are the *Aghios Efstratios* and *Lemnos* CSSs and the *Samothraki* ISS

6.1. South Chalkidiki offshore CSS (Athos ISS)

The *South Chalkidiki offshore* CSS represents the northern boundary of the NAB (Fig. 6). Its trace runs immediately south of the Sithonia and Athos peninsulae forming a NE-SW trending steep submarine slope for a total length of *ca.* 90 km as documented by bathymetric surveys (Maley and Johnson, 1971; Papanikolaou *et al.*, 2002) and seismic profiles (Ferentinos *et al.*, 1981; Roussos and Lyssimachou, 1991; Papanikolaou *et al.*, 2006). Based on slight strike variations and especially on the

occurrence of a strong earthquake likely associated with this fault zone, we distinguish the Athos ISS. The event occurred on November 8, 1905 and the macroseismic magnitude was 7.5 (Papazachos and Papazachou, 1997) or M_s = 7.3 (Ambraseys, 2001). This fault segment is *ca.* 54 km-long (Papanikolaou *et al.*, 2006). The maximum expected magnitude for the whole CSS is between 6.9 and possibly 7.5 as worst case scenario.

6.2. North Aegean Basin CSS

The *North Aegean Basin* CSS is one of the longest structures of the region with its *ca.* 140 km-length (Fig. 6). It strikes NE-SW and represents the southern boundary of the NAB, running from north of Limnos to the Sporades Islands. The fault zone is well expressed morphologically, as it has formed a deep and steep NW-dipping slope, clearly imaged in detailed bathymetric maps (Maley and Johnson, 1971; IOC, 1981; Papanikolaou *et al.*, 2002). The cumulative downthrown of the the sea-bottom is *ca.* 1300 m. The fault zone is also clearly imaged in the seismic reflection profiles indicating significant cumulative displacements and especially the deformation of the sea-bottom sediments (Brooks and Ferentinos, 1980; Ferentinos *et al.*, 1981; Mascle and Martin, 1990; Roussos and Lyssimachou, 1991; Papanikolaou *et al.*, 2006). Along this zone, two strong earthquakes, likely produced by two adjacent fault segments, are well-documented. Accordingly, we distinguish two ISSs: *Segment A* and *Segment B*, east and west, respectively).

Segment A ISS was responsible for the August 6, 1983 (M_w = 6.7) earthquake that reactivated the northeastern portion of the North Aegean Basin CSS. Based on the aftershock spatial distribution (Rocca *et al.*, 1985; Taymaz *et al.*, 1991) and the magnitude of the main shock, a length of 44 km is inferred. *Segment B* ISS is associated with the January 18, 1982 (M_w = 6.6) earthquake. Again, a length of 33 km is inferred from the aftershock spatial distribution (Taymaz *et al.*, 1991) and the magnitude of the main shock. There are many other focal mechanisms calculated for both 1982 and 1983 seismic crises (Dziewonski *et al.*, 1984; Papazachos *et al.*, 1984; Rocca *et al.*, 1985; Ekström *et al.*, 1987; Ekström and England, 1989; Kiratzi *et al.*, 1991; Taymaz *et al.*, 1991; Jackson *et al.*, 1992; Vannucci and Gasperini, 2003; 2004) all suggesting a very steep (NW-dipping) to sub-vertical nodal planes and an almost pure right-lateral strike-slip kinematics. The proposed segmentation is in agreement with the seismogenic source segments proposed by Papanikolaou and Papanikolaou (2007). The inferred mean displacement of the two segments is 0.88 m and 0.71 m (Segment A and Segment B, respectively). The 1982 and 1983 events likely represent the maximum expected magnitudes for the two segments, while in case of a unique rupture event (worst case scenario) the expected magnitude is 7.4 (Papanikolaou and Papanikolaou, 2007).

6.3. South NAT CSS

The South NAT CSS is probably the longest active structure affecting the Aegean Sea (Fig. 6). It is oriented ENE-WSW, running north of Limnos and Imbros Islands and controlling the Saros Gulf

(Armijo *et al.*, 1999; Kiratzi, 1991; Koral *et al.*, 2009; Koukouvelas and Aydin, 2002; Lybéris, 1984; McNeill *et al.*, 2004; Mercier *et al.*, 1989; Papadimitriou and Sykes, 2001; Saatçilar *et al.*, 1999; Stanley and Perissoratis, 1977). Although the structure is likely in mechanical continuity with the fault segment of the North Anatolian Fault which ruptured the Callipoli peninsula (August 9, 1912; M_w = 7.4), crossing it from the Saros Gulf to the Marmara Sea (Ambraseys and Finkel, 1987; Altunel *et al.*, 2004; Ambraseys, 2002; Janssen *et al.*, 2009; Kaya *et al.*, 2004; Rockwell *et al.*, 2001; Tüysüz *et al.*, 1998; Yaltirak and Alpar, 2002; Yaltirak *et al.*, 1998), we will not discuss further east in the frame of this paper. The fault zone geometry is relatively well constrained based on bathymetric data, seismic reflection profiles, microseismicity distribution, focal mechanism of moderate and strong events (Maley and Johnson, 1971; Mascle and Martin, 1990; Çagatay *et al.*, 1998; Coskun, 2000; Kurt *et al.*, 2000; Ustaömer et al, 2008; Papazachos *et al.*, 1991; Kiratzi *et al.*, 1991; McNeill *et al.*, 2004; Saatçilar *et al.*, 1999; Taymaz *et al.*, 1991; Karabulut *et al.*, 2006). Focal mechanisms document a prevailing strike-slip kinematics with some dip-slip component, while the distribution of the microseismicity suggests a high-angle (to sub-vertical) fault plane. The total length of the fault zone is probably more than 200 km. Based on the overall geometry, several segments certainly occur but the lack of specific data do not allow to determine the segment boundaries and especially their nature. Accordingly, the maximum expected magnitude could range between 6.5 and probably more then 7.5.

6.4. North NAT CSS

Mechanically associated with the South NAT CSS (see § 6.3) is the North NAT CSS, which runs subparallel and antithetic (SSE-dipping) to the former (Fig. 6). The two fault zones progressively converge eastwards probably merging into a unique crustal-scale flower structure at the entrance of the Saros Gulf (Çagatay *et al.*, 1998; Coskun, 2000; Kurt *et al.*, 2000; Yaltirak and Alpar, 2002; Yaltirak *et al.*, 1998). The total length is more than 120 km and the kinematics is oblique-slip (to strike-slip), according to available focal mechanism of moderate to strong events. Based on the slightly articulated geometry, at least two segments have been recognized and included in GreDaSS: the 26 km-long Saros ISS and the 24 km-long Samothraki SE ISS. Both faults have been reactivated by a M_w = 6.6 and M_w= 5.7 earthquakes occurred on March 27, 1975 and July 6, 2003, respectively north of the Callipoli peninsula and east of Samothraki Island (Kiratzi *et al.*, 1985; Taymaz *et al.*, 1991; Papazachos *et al.*, 1991; Jackson *et al.*, 1992; Papazachos and Papazachou, 1997; Vannucci and Gasperini, 2003; 2004; Karabulut *et al.*, 2006). Focal mechanisms suggest an oblique-slip motion (normal and dextral components) on a SE-dipping with medium dip-angle fault plane for the Saros ISS (Kiratzi *et al.*, 1985; Taymaz *et al.*, 1991; Papazachos *et al.*, 1991; Jackson *et al.*, 1992) and an almost pure dextral strike-slip motion on a steeply SE-dipping fault plane for the Samothraki SE ISS (Karabulut *et al.*, 2006). The investigation of the 2003 sequence (Karabulut *et al.*, 2006) indicates a thick seismogenic layer of *ca.* 19 km. Two historical strong events are also reported in this area (Papazchos and Papazachou, 1997): the first on July 23, 1719 (Me = 6.7) and the second on August 6,

1860 (M_e = 6.2). Although both events cannot be accurately located, at least one could be related with the Samothraki SE fault segment. A tentative value for the maximum expected magnitude is probably between 6.5 and 7.0.

6.5. North Samothraki ISS

The fault crosses the northern coast of the Samothraki Island and continues on both sides offshore (Fig. 6). From a mechanical point of view, this fault can be interpreted as a normal dip-slip secondary structure of the NAT. According to morphotectonic investigations the fault is characterized by discrete scarps most of them aligned in an ESE-WNW direction and dipping northwards (Pavlides *et al.*, 2005). They form a steep morphology that controls drainage and cause deposition of massive colluvial and alluvial deposits. The Samothraki ISS is probably the causative structure for the homonymous earthquake occurred on February 9, 1893 (Papazachos and Papazachos, 1997; Ambraseys, 2009). Based on the estimated macroseismic magnitude of 6.8 (Papazachos and Papazachos, 1997), the proposed length is at least 22 km.

6.6. Lemnos CSS

Lemnos CSS is a *ca.* 40 km-long, NE-SW-striking, sub-vertical strike-slip right-lateral structure running across the homonymous island (Fig. 6; Koukouvelas and Aydin, 2002; Pavlides *et al.*, 2009). It consists of several smaller segments, some of them controlling the coastline of the northeastern part of the island. The location, geometry and kinematics of this structure imply a possible connection with the South NAT CSS to the north. Even though regional instrumental seismicity is rather low, a strong (M_e = 7.0) historical (197 BC) earthquake is reported in the catalogue of Papazachos and Papazachou (1997) based on scripts of Pausanias, who refers to the sinking of Chryse Island NE from Lemnos. According to the empirical relationships (Wells and Coppersmith, 1994) the maximum expected magnitude of a total rupture of the fault zone is estimated to 6.9.

6.7. Aghios Efstratios CSS

The Aghios Efstratios CSS is a NE-SW-striking, tectonic structure, running south of the Limnos Island and crossing the small Aghios Efstratios Island (Fig. 6). Although it is parallel to the North Aegean Basin CSS (see § 6.2) its kinematics is mainly transcurrent based on the available focal mechanism of the 1968 event which reactivated most of the structure (McKenzie, 1972; Kiratzi *et al.*, 1991; Taymaz *et al.*, 1991; Vannucci and Gasperini, 2003; 2004). The field mapping indicates a NW-dipping high-angle to sub-vertical fault with significant right-lateral motion (Pavlides *et al.*, 1990; Pavlides and Tranos, 1991). The source dimensions (length of 75 km, width of 15 km) and an average displacement of 1.8 m are mainly based on the M_s = 7.1 magnitude of the 1968 earthquake (North, 1977). These values are in good agreement with the aftershock spatial distribution (Drakopoulos and Economides, 1972), though more recent papers (Nalbant *et al.*, 1998; Papadimitriou and Sykes, 2001) suggest different dimensions and displacement (see discussion in Pavlides *et al.*, 2009).

7. The Thessalian fault system

The first-order orographic texture of Thessaly is characterized by a NW-SE-trending basin-and-range-like tectonic system of latest Miocene-Early Pleistocene age, affecting the region between the Pindos mountain chain, to the west, and the Aegean Sea, to the east (Fig. 7). However, since Middle Pleistocene the area is undergoing a N(NE)-S(SW) stretching regime that created mainly normal E-W-tending fault systems generally overprinting the older basins but locally exploiting inherited structures (Caputo and Pavlides, 1991; 1993). As a consequence, the mean direction of the active faults is (E)SE-(W)NW. On land, structures are concentrated in the northern Larissa plain where they form the Tyrnavos Basin-Gonnoi Horst (*South Tyrnavos Basin*, *Tyrnavos*, *North Tyrnavos Basin* and *Omolio* CSSs) and in southern Thessaly (*Pagasitikos*, *Vasilika* and *Domokos* CSSs) generating an almost continuous belt from the Pagasitikos Gulf, to the east, to the Karditsa plain, to the west (Caputo, 1995). There is an important differentiation though, between the northern and southern sectors. Indeed, southern Thessaly has been struck by several strong earthquakes during historical as well as instrumental recording period (Papadopoulos, 1992), while in northern Thessaly no strong events have occurred during the last 2-3 centuries, with the only exception of the 1941 Larissa earthquake (Caputo and Helly, 2005a). Nevertheless, geological, paleoseismological, archaeoseismological and morphotectonic investigations clearly document the occurrence of strong linear morphogenic events also in the Tyrnavos Basin (Caputo *et al.*, 1994; 2003; 2004a). Based on this difference a seismic gap in northern Thessaly has been suggested (Caputo, 1995).

Three more CSSs belong to this geodynamic sector, which thus extends eastwards offshore the Thessalian coast (*South Cassandra offshore*, *Mavrovouni offshore* and *Pelion offshore* CSSs). These seismogenic sources are grouped here because of their parallelism with those onland and especially due to the sharp angular relationship with the CSSs described in the Northern Aegean offshore system (see chapter 6).

7.1. Pagasitikos CSS (Volos and Nea Anchialos ISSs)

As above mentioned, the southern Thessaly fault belt consists of three major CSSs. The easternmost is the ENE-WSW trending Pagasitikos CSS (Fig. 7). It dips southwards, controlling the northern coastline of the homonymous gulf and the margin of the Almyros Basin. Its total length is estimated to *ca.* 50 km, taking into account that the zone probably extends further to the east, across the southern Pelion peninsula. The morphological expression of the fault zone and its morphotectonic features as well as the two strongest events of the 1980 Magnesia earthquake sequence, document the existence of two distinct segments (*Volos* and *Nea Anchialos* ISSs) with a right-stepping partly overlapping geometry.

The *Volos* ISS is the eastern segment, almost totally lying offshore and controlling the northern coastline of the gulf. Morphological indications suggest onshore continuation across the Pelion

peninsula reaching a total length of 21 km. The roughly E-W-trending fault scarp is well-documented on the sea-floor from bathymetric surveys, seismic profiles and Holocene sediment distribution (Perissoratis *et al.*, 1991). The Volos ISS is responsible for the first strong shock (M_w = 6.5; July 9) of the 1980 seismic sequence. Calculated focal mechanisms of both the 1980 sequence and the April 30, 1985 (M_s = 5.5) event (Jackson *et al.*, 1982; Papazachos *et al.*, 1983; Dziewonski *et al.*, 1988; Ekström and England, 1989; Taymaz *et al.*, 1991; Vannucci and Gasperini, 2003; 2004) generally fit the geological observations, showing ENE-WSW-striking planes, shallow-dipping towards SSE with a normal dip-slip kinematics. A mean displacement of 0.63 m is estimated from empirical relationships. The 1980, M_w = 6.5 event likely represents the maximum expected magnitude.

The western segment of the fault zone is the *Nea Anchialos* ISS, which borders the northern margin of Almyros Basin partly controlling the northern coastline of the Pagasitikos Gulf. It has a total length of 23 km. It is the causative fault of the second strong shock (M_w = 6.1) of the 1980 sequence which occurred 24 minutes after the first one, suggesting a triggering phenomenon. The mapped fault trace and coseismic ruptures (Papazachos *et al.*, 1983; Ambraseys and Jackson, 1990; Caputo, 1996) indicate an ENE-WSW strike and a SSE dip-angle (Papazachos *et al.*, 1983; Caputo and Pavlides, 1991; Mountrakis *et al.*, 1993a; Caputo, 1995; 1996; Galanakis *et al.*, 1998; Zovoili *et al.*, 2004). Microearthquake surveys (Kementzetzidou, 1996; Hatzfeld *et al.*, 1999), delineate a south-dipping fault plane (*ca.* 55°) and a seismogenic layer thickness of *ca.* 12 km. Both meso-structural analyses (Caputo and Pavlides, 1991; 1993; Caputo, 1996) and focal mechanisms (Jackson *et al.*, 1982; Papazachos *et al.*, 1983; Dziewonski *et al.*, 1988; Ekström and England, 1989; Taymaz *et al.*, 1991; Vannucci and Gasperini, 2003; 2004) indicate normal faulting associated with a N-S stretching direction. Based on geomorphic markers, a slip-rate between 1 and 3 mm/a is estimated (Caputo, 1996) and a recurrence interval of 1500 years is suggested (Zovoili *et al.*, 2004).

7.2. Vasilika CSS (Righeo and Dasolofos ISSs)

NW of the Pagasitikos CSS (see §7.1) is the Vasilika CSS which obliquely crosses the Pliocene-Early Pleistocene Central Hills horst in an E-W to ESE-WNW direction drawing a slightly curved fault trace (Fig. 7; Caputo, 1996). The fault zone disappears under the Quaternary sediments of the Karditsa plain being uncertain its westward continuation. The mapped neotectonic fault length is *ca.* 64 km. In the central-eastern sector, two major fault segments have been recognized (Caputo, 1995): *Righeo* and *Dasolofos* ISSs, east and west respectively. The two segments have left-stepping partly overlapping geometry and show clear morphotectonic evidences affecting Late Pleistocene deposits (Caputo, 1995; Caputo and Pavlides 1993). Mesostructural analyses indicate a SSW-dipping setting and a normal dip-slip kinematics compatible with a roughly N-S direction of extension. The Righeo ISS is 22 km-long, while the Dasolofos is 15 km. A microearthquake cluster has been instrumentally recorded within the seismogenic volume thus documenting a seismogenic depth of at least 12-13 km and 60°-70° of mean dip-angle (Kementzetzidou, 1996; Hatzfeld *et al.*, 1999). On March 8, 1957 two

strong shocks (M_s = 6.5 and 6.6 respectively, according to Ambraseys and Jackson, 1990, or M_w = 6.4 according to Vannucci and Gasperini, 2003; 2004) occurred near Velestino. They have been associated with this fault zone (Caputo, 1995). Although the poor seismological recordings and especially the time difference of 7 min between the two shocks hamper a separate reconstruction of the two macroseismic fields, a possible triggering effect could be tentatively suggested. Considering the magnitudes, it is likely that both segments were (partly) reactivated. Ground ruptures are reported by local people only along the Righeo ISS (Ambraseys and Jackson, 1990). The mean displacements are estimated to 0.8 m and 0.6 m and the maximum expected magnitudes to 6.7 and 6.5, for the two ISSs respectively.

7.3. Domokos CSS (Ekkara ISS)

The westernmost seismogenic structure of the southern Thessaly fault belt is represented by the Domokos CSS (Fig. 7), which shows an antithetic setting (*i.e.* NNE-dipping) with respect to the Pagasitikos and Vasilika CSSs (see §§7.1-7.2). The fault trace is marked by a curvilinear scarp, varying in strike between E-W and (W)NW-(E)SE, from east to west, due to the linkage of inherited structures (the latter trend) with recently created ones (the former). Based on geological and morphotectonic investigations (Caputo and Pavlides, 1993; Pavlides, 1993), the total length can be roughly estimated to 48 km, while mesostructural analyses document dip-slip to oblique-slip kinematics compatible with a NNE-SSW stretching direction (Caputo, 1995). The central sector of the fault zone (*Ekkara* ISS) was reactivated by the April 30, 1954, Sophades earthquake that produced several km-long ground ruptures (Papastamatiou and Mouyiaris, 1986). The initially assessed surface magnitude was 7.0 (Papastamatiou and Mouyiaris, 1986), but it is likely overestimated (M_s = 6.7, Ambraseys and Jackson, 1990; M_w = 6.6, Vannucci and Gasperini, 2003; 2004). Recent palaeoseismological investigations clearly document that this structure was already reactivated in the past and suggest a minimum slip-rate of 0.3-0.5 mm/a and a recurrence interval greater than 3 ka (Palyvos *et al.*, 2010). The total length of the Ekkara ISS is estimated to 30 km. The focal mechanism proposed by Vannucci and Gasperini (2003; 2004) suggests a WNW-tending NNE-dipping rupture plane, which is slightly different from that proposed by McKenzie (1972).

7.4. South Tyrnavos Basin CSS (Larissa and Asmaki ISSs)

As mentioned above, northern Thessaly is characterized by very low historical and instrumental seismicity, but prominent neotectonic structures showing evidences of recent activity. The geological similarity and the contrasting seismological record suggest the occurrence of a seismic gap in the northern Larissa plain (Caputo, 1995). One of these neotectonic structures is the South Tyrnavos Basin CSS (Fig. 7) bordering to the south the homonymous graben and showing a NNE-dipping setting with a normal dip-slip kinematics (Caputo *et al.*, 1994). The fault zone is *ca.* 40 km-long. Two segments have been recognized: *Larissa* and *Asmaki* ISSs (west and east respectively).

The *Larissa* ISS forms a noticeable fault scarp separating the Pliocene-Early Pleistocene deposits of the Central Hills (footwall) from the recent alluvial sediments of the Pinios River (hanging-wall). Based on geological and morphotectonic investigations as well as geophysical surveys (Caputo and Pavlides, 1993; Caputo *et al.*, 2003) the fault has a length of 19 km and a mean ESE-WNW orientation. The eastern tip corresponds to an angular barrier and a left-stepping underlapping geometry with the nearby structure. Based on empirical relationships, the maximum expected magnitude is estimated to 6.6, while the slip-rate ranges between 0.1 and 0.5 mm/a (Caputo, 1995).

In the eastern sector, morphological evidence is more subtle probably due to an overall lower slip-rate. However, recent tectonic activity is well documented by the occurrence of few meters-high, but several km-long, E-W trending scarps affecting the Holocene sediments of the Larissa plain (Caputo *et al.*, 1994) and documenting three sub-parallel overlapping sub-emergent fault planes. One of these structures (*Asmaki* ISS) is *ca.* 11 km-long and has been probably reactivated by the March 1, 1941 Larissa earthquake based on the occurrence of co-seismic ground ruptures along one of these morphological alignments (Ambraseys and Jackson, 1990; Caputo, 1995). The focal mechanism indicates a NNE-dipping slightly oblique-slip nodal plane, while the magnitude of this event is M_w = 6.1 (Vanucci and Gasperini, 2003; 2004; M_e = 6.3 according to Papazachos and Papazachou, 1997). Although the eastern sector of the South Tyrnavos Basin CSS is longer than the Asmaki Fault, due to the above mentioned slip partitioning the 1941 possibly represents the maximum expected magnitude.

7.5. Tyrnavos CSS (Tyrnavos ISS)

The Tyrnavos CSS (Fig. 7) is parallel to and synthetic with the South Tyrnavos Basin CSS (see §7.4). With the latter structure forms a largely overlapping right-stepping geometry. It trends ESE-WNW showing a total length of at least 20 km. The well defined section of the fault is constrained to a length of 14 km and is conservatively represented by the *Tyrnavos* ISS which forms a prominent scarp affecting the Triassic rocks as well as Pliocene and Late Quaternary sediments (Caputo, 1993a; 1995). A continuous unweathered fresh scarp and 10-15 cm-high free-faces likely document recent co-seismic reactivations (Caputo, 1993a). The displacement of latest Pleistocene-Holocene alluvial deposits along a 8-10 m-high scarp as well as borehole data suggest a long-term slip-rate ranging between 0.1 and 0.4 mm/a (Caputo, 1993b; Caputo *et al.*, 2004a; 2006). The fault surface has been also detected from geophysical surveys: GPR (Caputo and Helly, 2000), ERTs (Caputo *et al.*, 2003) and HSVR (Oliveto *et al.*, 2004). The results of several palaeoseismological trenches document the occurrence of at least 12-13 events during the last 25-30 ka and a mean recurrence interval of 1.5-2.5 ka (Caputo and Helly, 2007). The maximum expected magnitude for the ISS is *ca* 6.3, while if the whole CSS is reactivated it could generate a 6.7 event.

7.6. North Tyrnavos Basin CSS (Rodia and Gyrtoni ISSs)

The Tyrnavos Basin is bounded to the north by another major CSS (North Tyrnavos Basin)

antithetic to and facing the previosuly described ones (Fig. 7). The fault zone is characterized by an articulated geometry due to the linkage of inherited NW-SE tending segments and newly formed E(SE)-W(NW) tending ones (Caputo, 1993b; Caputo and Helly, 2005b). Geological, structural, morphotectonic and geophysical investigations allowed to map the CSS in detail and document its recent activity (Caputo, 1993b; 1995; Caputo and Pavlides, 1993; Caputo *et al.*, 1994; 2003), which is further confirmed by the results of palaeoseismological trenches (Caputo and Helly, 2000; 2005b; Caputo *et al.*, 2004b). Mesostructural analyses indicate a NNE-SSW direction of extension (Caputo, 1993b). The total length of this fault zone is *ca.* 47 km. There are two major recognized fault segments: *Rodia* and *Gyrtoni* ISSs (Caputo, 1993b; 1995; Caputo and Pavlides, 1993; Caputo *et al.*, 1994; Goldsworthy and Jackson, 2000) bearing the best evidence of recent activity.

The *Rodia* Fault is 15 km-long and trends in an ESE-WNW direction. It separates the Palaeozoic metamorphic rocks of the Pelagonian Zone, to the north, from the Pleistocene and Holocene sediments, to the south. The latters consist of scree deposits coming from the mountain front interfingering with the alluvial ones of the Pinios River. Palaeoseismological investigations document a Holocene linear morphogenic earthquake dated 2-3 ka BP with a vertical displacement 25-30 cm and a possible magnitude of 6.4 ±0.2 (Caputo and Helly, 2005b). With the addition of morphotectonic and stratigraphic data, a slip-rate ranging between 0.1 and 1.0 mm/a has been suggested.

The *Gyrtoni* Fault is parallel to and synthetic with the Rodia ISS showing a right-stepping underlapping geometry. The fault is 13 km-long and mainly marked by a morphological scarp separating Villafranchian lacustrine deposits (footwall) from Holocene alluvial sediments (Caputo *et al.*, 1994). Further evidence of its recent activity comes from high-resolution geophysical investigations (Caputo *et al.*, 2003).

The seismogenic layer thickness of the area is assumed 12.5 km by interpolation between the areas of the Aliakmonas and Pagasitikos CSSs. The maximum expected magnitudes of Rodia and Gyrtoni faults are 6.3 and 6.1, respectively, with a corresponding co-seismic mean displacement of 0.3 m. The complex geometry of the CSS rejects scenarios of total rupturing.

7.7. Omolio CSS

The Omolio CSS is the northernmost active structure of the Thessalian fault system (Fig. 7). It is ESE-WNW trending, NNE-dipping and separates the Palaeozoic-Mesozoic bedrock from the Holocene alluvial and deltaic deposits of the Pinios River (eastern sector; Caputo, 1990). Together with the antithetic and diverging North Tyrnavos Basin CSS (see §7.6) it delimits the Gonnoi Horst, which was strongly uplifted in recent times (Stiros *et al.*, 2004). The fault zone showing a recent tectonic activity, like a major linear escarpment and several suspended valleys, has a total length of *ca.* 38 km. On June 9, 2003 a moderate earthquake (M_w = 5.3) hit the area, showing a coherent focal mechanism (Pavlides *et al.*, 2004b) The event was probably associated with this seismogenic volume, but too deep and small to produce a clear surface expression. In case a large part of the CSS is

reactivated, a maximum magnitude of 6.5 could be expected.

7.8. South Kassandra offshore CSS

The *South Kassandra offshore* CSS is the western continuation of the South Chalkidiki offshore CSS (see § 6.1), but characterized by a marked orientation change along strike, from E-W to ESE-WNW (Fig. 7). The total length is 46 km and the kinematics is likely pure dip-slip normal (Papanikolaou *et al.*, 2002). It forms a major submarine escarpent following the coastline of the Kassandra peninsula, while its recent activity is inferred from high-resolution seismic reflection profiles (Papanikolaou *et al.*, 2006), which show a clear downthrow of the southern block and the deformation of the sea-floor sediments.

7.9. Pelion offshore CSS

The southwestern border of the NAB, offshore the eastern Pelion peninsula and north of Skiathos and Skopelos Islands, is represented by a (W)NW-(E)SE trending fault zone (Fig. 7). This tectonic structure is *ca.* 36 km-long and NE-dipping as emphasized by a steep morphological submarine slope (Papanikolaou *et al.*, 2002). The location and geometry of the fault zone and its recent activity is also clear in the seismic reflection profiles showing that it displaces and deforms the sea-bottom sediments (Laigle *et al.*, 2000; Papanikolaou *et al.*, 2006). Based on its orientation and the geodynamic setting, the kinematics should be slightly oblique-slip, but with a prevailing normal dip-slip component.

8. Concluding remarks

Since the beginning of the GreDaSS Project, more than 35 CSSs and 55 ISSs have been recognized, studied and analyzed in the pilot area of North Greece, while many seismogenic sources are in progress for the rest of the Greek territory. Several ISSs have been directly and confidently associated with recent instrumentally recorded earthquakes, even more have been related with historical events and many have been recognized as individual segments. The greatest majority of ISSs belongs to larger fault zones represented by CSSs. A key-feature of GreDaSS is the 3D representation and parameterization of the active faults from which large seismogenic volumes can be defined that can help to understand the ongoing geodynamic processes affecting the Aegean crust.

Based on the 3D structure (geometry) of many seismogenic sources, observations on the fault clustering and regional pattern, the homogeneity of data concerning the kinematic behaviour, and the comparison of similar well known structures out of, but near to, the study area (*i.e.* the Gulf of Corinth), the occurrence of several low-angle normal detachment fault zones can be inferred for the mainland of North Greece (Sboras and Caputo, 2010). For example, the fault system of the Mygdonia Basin probably roots from the N-dipping low-angle shear zone of the Anthemountas CSSs (Tranos *et al.*, 2003). Similarly, in the Kozani area, the Palaeochori ISS can be interpreted as a northern splay of the shallow NNW-dipping structure of Deskati DSS (Chiarabba and Selvaggi, 1997; Hatzfeld *et al.*, 1997; 1998; Doutsos and Koukouvelas, 1998). A comparable geological and tectonic setting can be envisaged for the Ptolemaida Basin (Sboras and Caputo, 2010).

Moreover, the homogenization process during data collection and parameterization of the seismogenic sources in the database allowed us to roughly distinguish five sectors showing common geometrical and geodynamic characteristics: i) a northern E-W trending fault belt in Thrace and Eastern Macedonia, ii) a complex E(SE)-W(NW) trending fault system affecting the Chalkidiki peninsula and possibly associated with low-angle detachments, iii) the NE-SW trending anti-Hellenic fault system in Western Macedonia and Epirus, iv) the E(SE)-W(NW) trending Thessalian fault system and v) the (E)NE-(W)SW trending North Aegean fault system, which is almost exclusively located offshore. These sectors likely correspond to major crustal (and lithospheric?) blocks characterized by partially independent behaviour at least during Quaternary, but they could be also associated with the occurrence of older inherited structures.

This paper attempts to make a contribution towards synthesizing and standardizing published and new data, aiming at a more precise seismic hazard assessment for northern Greece and assist the refinement of the current seismic zonation of the area.

Acknowledgments

References

Altunel E., Meghraoui M., Akyüz H.S. and Dikbas A. (2004): Characteristics of the 1912 co-seismic rupture along the North Anatolian Fault Zone (Turkey): implications for the expected Marmara earthquake. *Terra Nova*, **16**, 198-204.

Ambraseys N. (1999): Early earthquakes in the Kozani Area, northern Greece. *Tectonophysics*, **308**, 291-298.

Ambraseys N.N. (2001): Reassessment of earthquakes, 1900-1999, in the Eastern Mediterranean and the Middle East. *Geophys. J. Int.*, **145**, 471-485.

Ambraseys N. (2002): The Seismic Activity of the Marmara Sea Region over the Last 2000 Years. *Bull. Seism. Soc. Am.*, **92**, 1-18.

Ambraseys N. (2009): *Earthquakes in the Mediterranean and Middle East: A Multidisciplinary Study of Seismicity up to 1900*. Cambridge University Press, Cambridge, 968 pp.

Ambraseys N.N. and Finkel C.F. (1987): The Saros-Marmara earthquake of 9 August 1912. *Earthq. Eng. Struct. Dyn.*, **15**, 189-211.

Ambraseys N.N. and Jackson J.A. (1990): Seismicity and associated strain of central Greece between 1890 and 1988. *Geophys. J. Int.*, **101**, 663-708.

Ambraseys N.N. and Jackson J.A. (1998): Faulting associated with historical and recent earthquakes in the Eastern Mediterranean region. *Geophys. J. Int.*, **133**, 390-406.

Anderson H. and Jackson J. (1987): Active tectonics of the Adriatic Region. *Geophys. J. R. astr. Soc.*, **91**, 937-983.

Armijo R., Meyer B., Hubert A. and Barka A. (1999): Westward propagation of the North Anatolian fault into the northern Aegean: Timing and kinematics. *Geology*, **27**, 267-270.

Atzemoglou A., Tsourlos P. and Pavlides S. (2003): Investigation of the Tectonic Structure of the NW Part of the Amynteon Basin (NW Greece) by means of a Vertical Electrical Sounding (VES) survey. *J. Balkan Geophys. Soc.*, **6**(4), 188-201.

Baker C., Hatzfeld D., Lyon-Caen H., Papadimitriou E. and Rigo A. (1997): Earthquake mechanisms of the Adriatic Sea and western Greece. *Geophys. J. Int.*, **131**, 559-594.

Barker J. S. and Langston C.A. (1981): Inversion of teleseismic body waves for the moment tensor of the 1978 Thessaloniki, Greece, earthquake. *Bull. Seism. Soc. Am.*, **71**, 1423-1444.

Basili R., Valensise G., Vannoli P., Burrato P., Fracassi U., Mariano S., Tiberti M.M., Boschi E. (2008): The database of individual seismogenic sources (DISS), version 3: summarizing 20 years of research on Italy's Earthquake Geology. *Tectonophysics*, **453**(1-4), 20-43.

Boccaletti M., Caputo R., Mountrakis D., Pavlides S. and Zouros N. (1997): Paleoseismicity of the Souli Fault, Epirus, Western Greece, *J. Geodynamics*, **24**(1-4), pp. 117-127.

Brooks M. and Ferentinos G. (1980): Structure and evolution of the Sporadhes basin of the North Aegean trough. *Tectonophysics*, **68**, 15-30.

Caputo R. (1993a): Morphotectonics and kinematics of the Tyrnavos Fault, northern Larissa plain, Greece. *Z. Geomorph. N. E.*, **94**, 167-185.

Caputo R. (1993b): The Rodia fault system: an active complex shear zone (Larissa plain, Central Greece). *Bull. Geol. Soc. Greece*, **28**(1), 447-456.

Caputo R. (1995): Inference of a seismic gap from geological data: Thessaly (Central Greece) as a case study. *Ann. Geofisica*, **38**, 1-19.

Caputo R. (1996): The active Nea Anchialos Fault System (Central Greece): comparison of geological, morphotectonic, archaeological and seismological data. *Ann. Geofisica*, **39**(3), 557-574.

Caputo R. and Helly B. (2000): Archéosismicité de l'Égée: étude des failles actives de la Thessalie. *Bull. Corresp. Hell.*, **124**(2), 560-588.

Caputo R. and Helly B. (2005a): Archaeological evidences of past earthquakes: a contribution to the SHA of Thessaly, Central Greece. *J. Earthq. Eng.*, **9**(2), 199-222.

Caputo R. and Helly B. (2005b): The Holocene activity of the Rodia Fault, Central Greece. *J. Geodynamics*, **40**, 153-169.

Caputo R. and Helly B. (2007): The European Palaeoseismological Museum of Tyrnavos, Central Greece. EGU General Assembly, Vienna, April 16-20, 2007, *Geophysical Research Abstracts*, **9**, 00283

Caputo R. and Pavlides S. (1991): Neotectonics and structural evolution of Thessaly (Central Greece). *Bull. Geol. Soc. Greece*, **25**(3), 119-133.

Caputo R. and Pavlides S. (1993): Late Cainozoic geodynamic evolution of Thessaly and surroundings (central-northern Greece). *Tectonophysics*, **223**, 339-362.

Caputo R. and Zouros N. (1993): Examples of Alpide deformation from Epirus: local anomalies or need to re-evaluate the amount of shortening in the Western Hellenides?, *Bull. Geol. Soc. Greece*, **28**(1), 315-326.

Caputo R., Bravard J.-P. and Helly B. (1994): The Pliocene-Quaternary tecto-sedimentary evolution of the Larissa Plain (Eastern Thessaly, Greece). *Geodinamica Acta*, **7**(4), 219-231.

Caputo R., Piscitelli S., Oliveto A., Rizzo E. and Lapenna V. (2003): The use of electrical resistivity tomography in Active Tectonic. Examples from the Tyrnavos Basin, Greece. *J. Geodyn.*, **36**(1–2), 19-35.

Caputo R., Helly B., Pavlides S. and Papadopoulos G. (2004a): Palaeoseismological investigation of the Tyrnavos Fault (Thessaly, Central Greece). *Tectonophysics*, **394**, 1-20.

Caputo R., Oliveto A. and Helly B. (2004b): Palaeoseismological researches along the Rodia Fault, Central Greece. Proceedings of 5th International Symposium on Eastern Mediterranean Geology, 14-20 April 2004, Thessaloniki, Greece, Ref: S2-6.

Caputo R., Helly B. Pavlides S. and Papadopoulos G. (2006): Archaeo- and palaeoseismological investigations in Northern Thessaly (Greece): Insights for the seismic potential of the region. *Nat. Hazards*, **39**, 195-212.

Caputo R., Pavlides S. and Mucciarelli M. (2008): Magnitude distribution of linear morphogenic earthquakes in the Mediterranean Region: insights from palaeoseismological and historical data. *Geophys. J. Int.*, **174**, 930-940, doi: 10.1111/j.1365-246X.2008.03834.x

Carver D. and Bollinger G.A. (1981): Aftershocks of the June 20, 1978 Greece earthquake: a multimode faulting sequence. *Tectonophysics*, **73**, 343-363.

Çagatay M.N., Görür N., Alpar B., Saatçilar R., Akkök R., Sakinç M., Yüce H., Yaltirak C. and Kuscu I. (1998): Geological evolution of the Gulf of Saros, NE Aegean Sea. *Geo-Mar. Lett.*, **18**, 1-9.

Chatzipetros A. (2008): *Paleoseismological and morphotectonic study of the active fault systems at Mygdonia basin, eastern Halkidiki and Kozani-Grevene.* PhD Thesis, Department of Geology, ristotle University of Thessaloniki, Greece, 354 pp.

Chatzipetros A. and Pavlides S. (2004): Geometry and kinematics of the Maronia-Makri active fault (Thrace, northeastern Greece). 4th National Geophysical Conference of the Bulgarian Geophysical Society, October 4-5, 2004, Sofia, Bulgaria, Session 1, 61-63.

Chatzipetros A.A., Pavlides S.B. and Mountrakis D.M. (1998): Understanding the 13 May 1995 western Macedonia earthquake: a paleoseismological approach. *J. Geodynamics*, **26**(2-4), 327-339.

Chatzipetros A., Pavlides S. and Mourouzidou O. (2004): Re-evaluation of Holocene earthquake activity in Mygdonia basin, Greece, based on new paleoseismological results. 5th Int. Symp. East. Mediterr. Geol., Ref: S2-15.

Chatzipetros A., Michailidou A., Tsapanos Th. and Pavlides S. (2005): Morphotectonics and seismotectonics of the Stratoni-Barbara and Gomati-Megali Panagia active fault (eastern Chalkidiki, Northern Greece). *Bull. Geol. Soc. Greece*, **XXXVII**, 127-142.

Cheng S., Fang Z., Pavlides S. and Chatzipetros A. (1994): Preliminary study of paleoseismicity of the southern Langada-Volvi basin margin fault zone, Thessaloniki, Greece. *Bull. Geol. Soc. Greece*, **30**(1), 401-407.

Chiarabba C. and Selvaggi G. (1997): Structural central on fault geometry: example of the Grevena Ms 6.6, normal faulting earthquake. *J. Geophys. Res.*, **102**, 22 445-22 457.

Coskun B. (2000): North Anatolian Fault-Saros Gulf relationships and their relevance to hydrocarbon exploration, northern Aegean Sea, Turkey. *Mar. Petrol. Geol.*, **17**, 751-772.

Diamantopoulos A. (2006): Plio–Quaternary Geometry and Kinematics of Ptolemais Basin (Northern Greece): Implications for the Intra-Plate Tectonics in Western Macedonia. Geologia Croatica, **59**(1), 85-96.

Doutsos T. and Kokkalas S. (2001): Stress and deformation patterns in the Aegean region. *J. Struct. Geol.*, **23**, pp. 455-472.

Doutsos T. and Koukouvelas I. (1998): Fractal analysis of normal faults in northwestern Aegean area, Greece. *J. Geodynamics*, **26**(2-4), 197-216.

Drakopoulos J.C. and Economides A.C. (1972): Aftershocks of February 19, 1968 earthquake in Northern Aegean Sea and related problems. *Pure Appl. Geophys.*, **95**, 100-115.

Dziewonski A.M., Friedman A., Giardini D. and Woodhouse J.H. (1983): Global seismicity of 1982: centroid-moment tensor solutions for 308 earthquakes. *Phys. Earth Planet. Inter.*, **33**, 76-90.

Dziewonski A.M., Franzen J.E. and Woodhouse J.H. (1984): Centroid-moment tensor solutions for July-September, 1983. *Phys. Earth Planet. Inter.*, **34**, 1-8.

Dziewonski A.M., Franzen J.E. and Woodhouse J.H. (1985): Centroid-moment tensor solutions for July-September, 1984. *Phys. Earth Planet. Inter.*, **38**, 203-213.

Dziewonski A.M., Franzen J.E. and Woodhouse J.H. (1986): Centroid-moment tensor solutions for October-December 1985. *Phys. Earth Planet. Inter.*, **43**, 185-195.

Dziewonski A.M., Ekström G., Franzen J.E. and Woodhouse, J.H. (1987): Global seismicity of 1978: centroid-moment tensor solutions for 512 earthquakes. *Phys. Earth Planet. Inter.*, **46**, 316-342.

Dziewonski A. M., Ekström G., Franzen J. E. and Woodhouse J. H. (1988): Global seismicity of 1980: centroid-moment tensor solutions for 515 earthquakes. *Phys. Earth Planet. Inter.*, **50**, 127-154.

Dziewonski A.M., Ekström G., Woodhouse J.H. and Zwart G. (1991): Centroid-moment tensor solutions for October–December 1990. *Phys. Earth Planet. Inter.*, **68**, 201-214.

Dziewonski A.M., Ekström G. and Salganik M.P. (1996): Centroid-moment tensor solutions for April-June 1995. *Phys. Earth Planet. Inter.*, **96**, 1-13.

Dziewonski A.M., Ekström G., Maternovskaya N.N. and Salganik M.P. (1997): Centroid-moment tensor solutions for July-September, 1996. *Phys. Earth Planet. Inter.*, **102**, 133-143.

Ekström G. and England P. (1989): Seismic Strain Rates in Regions of Distributed Continental Deformation. *J. Geophys. Res.J. Geophys. Res.*, **94**(B8), 10,231-10,257.

Ekström G., Dziewonski A.M. and Woodhouse J.H. (1987): Centroid-moment tensor solutions for the 51 IASPEI selected earthquakes, 1980-1984. *Phys. Earth Planet. Inter.*, **47**, 62-66.

Ferentinos G., Brooks M. And Collins M. (1981): Gravity-induced deformation on the north flank and floor of the Sporadhes Basin of the North Aegean Sea Trough. *Mar. Geol.Mar. Geol.*, **44**, 289-302.

Floras D. (1933): The destructions of the Chalkidiki earthquakes. *Tech. Chron.*, **25**, 21-28 (in Greek).

Galanakis D. Pavlides S. and Mountrakis D. (1998): Recent brittle tectonic in Almyros-Pagasitikos, Maliakos, N. Euboea & Pilio. *Bull. Geol. Soc. Greece*, **42**(1), 263-273.

Galanakis D., Paschos P., Rondoyanni T. and Georgiou C. (2007): Neotectonic Activity of Konitsa Area and the 1996 Earthquakes. *Hell. J. Geosciences*, **42**, 57-64.

Galanis O.C., Papazachos C.B., Hatzidimitriou P.M. and Scordilis E.M. (2004): Application of 3-D velocity models and ray tracing in double difference earthquake location algorithms: application to the Mygdonia basin (northern Greece). *Bull. Geol. Soc. Greece*, **36**(3), 1396-1405.

Ganas A., Pavlides S.B., Sboras S., Valkaniotis S., Papaioannou S., Alexandris G.A., Plessa A. and Papadopoulos G.A. (2004): Active fault geometry and kinematics in Parnitha Mountain, Attica, Greece. *J. Struct. Geol.*, **26**, 2103-2118.

Georgalas G. and Galanopoulos A. (1953): Das grosse Erdbeben der Chalkidike vom 26 September 1932. *Bull. Geol. Soc. Greece*, **1**, 11-63.

Goldsworthy M. and Jackson J. (2000): Active normal fault evolution in Greece revealed by geomorphology and drainage patterns. *Geol. Soc. LondonJ. Geol. Soc. London*, **157**, 967-981.

Goldsworthy M. and Jackson J. (2001): Migration of activity within normal fault systems: examples from the Quaternary of mainland Greece. *J. Struct. Geol.*, **23**, 489-506.

Goldsworthy M., Jackson J. and Haines J. (2002): The continuity of active fault systems in Greece. *Geophys. J. Int.*, **148**, pp. 596-618.

Guidoboni E. and Comastri A. (2005): Catalogue of earthquakes and tsunamis in the Mediterranean area from the 11th to the 15th century. INGV'SGA, Bologna, 1037 pp.

Guidoboni E., Comastri A. and Traina G. (1994): *Catalogue of ancient earthquakes in the Mediterranean area up to 10th century*. INGV-SGA, Bologna, 504 pp.

Hanks T.C. and Kanamori H. (1979): A moment magnitude scale. *J. Geophys. Res.*, **84**(B5), 2348-2350.

Hatzfeld D., Christodoulou A.A., Scordilis E.M., Panagiotopoulos D. and Hatzidimitriou P.M. (1986/87): A microearthquake study of the Mygdonian graben (northern Greece). *Earth Planet. Sci. Lett.Earth Planet. Sci. Lett.*, **81**, 379-396.

Hatzfeld D., Kassaras I., Panagiotopoulos D., Amorese D., Makropoulos K., Karakaisis G. and Coutant O. (1995): Microseimicity and strain pattern in northwestern Greece, *Tectonics*, **14**(4), 773-785

Hatzfeld D., Karakostas V., Ziazia M., Selvaggi G., Lebogne S., Berge C., Guiguet R., Paul A., Voidomatis, P., Diagourtas D., Kassaras I., Koutsikos I., Makropoulos K., Azzara R., Di Bona M., Baccheschi S., Bernard P. and Papaioannou C. (1997): The Kozani-Grevena (Greece) earthquake of 13 May 1995 revisited from a detailed seismological study. *Bull. Seism. Soc. Am.*, **87**(2), 463-473.

Hatzfeld D., Karakostas V., Ziazia M., Selvaggi G., Lebogne S., Berge C. and Makropoulos K. (1998): The Kozani-Grevena (Greece) earthquake of May 13, 1995, a seismological study. *J. Geodynamics*, **26**(2-4), 245-254.

Hatzfeld D., Ziazia M., Kementzetzidou D., Hatzidimitriou P., Panagiotopoulos D., Makropoulos K., Papadimitriou P. and Deschamps A. (1999): Microseismicity and focal mechanisms at the western termination of the North Anatolian Fault and their implications for continental tectonics. *Geophys. J. Int.*, **137**, 891-908.

IOC (Intergovernmental Oceanographic Commssion) (1981): International bathymetric chart of the Mediterranean. Head Department of Navigation and Oceanography, Ministry of Defence, Leningrand, USSR, 1st edition.

Jackson J.A., King G. and Vita-Finzi C. (1982): The neotectonics of the Aegean: an alternative view. *Earth Planet. Sci. Lett.Earth Planet. Sci. Lett.*, **61**, 303-318.

Jackson J., Haines J. and Holt W. (1992): The Horizontal Velocity Field in the Deforming Aegean Sea Region Determined From the Moment Tensors of Earthquakes. *J. Geophys. Res.J. Geophys. Res.*, **97**(B12), 17,657-17,684.

Janssen C., Bohnhoff M., Vapnik Y., Görgün E., Bulut F., Plessen B., Pohl D., Aktar M., Okay A.I. and Dresen G. (2009): Tectonic evolution of the Ganos segment of the North Anatolian Fault (NW Turkey). *J. Struct. Geol.*, **31**, 11-28.

Jenny S., Goes S., Giardini D. and Kahle H.-G. (2004): Earthquake recurrence parameters from seismic and geodetic strain rates in the eastern Mediterranean. *Geophys. J. Int.*, **157**, 1331-1347, doi: 10.1111/j.1365-246X.2004.02261.x.

Kanamori D.H. and Anderson D.L. (1975): Theoretical basis of some empirical relations in seismology. *Bull. Seismol. Soc. Am.*, **65**, 1073-1095.

Kaya Ş., Müftüoglu O. and Tüysüz O. (2004): Tracing the geometry of an active fault using remote sensing and digital elevation model: Ganos segment, North Anatolian Fault zone, Turkey. *Int. J. Remote Sens.*, **25**(19), 3843-3855.

Karabulut H., Roumelioti Z., Benetatos C., Mutlu A.K., Özalaybey S., Aktar M. and Kiratzi A. (2006): A source study of the 6 July 2003 (Mw 5.7) earthquake sequence in the Gulf of Saros (Northern Aegean Sea): Seismological evidence for the western continuation of the Ganos fault. *Tectonophysics*, **412**, 195-216.

Kementzetzidou D. (1996): *Étude sismotectonique du systéme Thessalie-iles Sporades (Gréce centrale)*. PhD Thesis, Observatoire de Grenoble, 151 pp.

King G., Tselentis A., Gomberg J., Molnar P., Roecker S., Sinvhal H., Soufleris C. and Stock J. (1983): Microearthquake seismicity and active tectonics of northwestern Greece. *Earth Plan. Sci. Lett.*, 66, 279-288.

Kiratzi A.A. (1991): Rates of Crustal Deformation in the North Aegean Trough-North Anatolian Fault Deduced from Seismicity. *PAGEOPH*, **136**(4), 421-432.

Kiratzi A.A. (1999): Stress tensor inversion in Western Greece using earthquake focal mechanisms from the Kozani-Grevena 1995 seismic sequence. *Ann. Geofis.*, **42**(4), 725-734.

Kiratzi A. (2010): The 24 May 2009 Mw5.2 earthquake sequence near Lake Doirani (FYROM-Greek borders): Focal mechanisms and slip model using empirical source time functions inversion. *Tectonophysics*, **490**, 115-122, doi:10.1016/j.tecto.2010.04.035.

Kiratzi A. and Louvari E. (2003): Focal mechanisms of shallow earthquakes in the Aegean Sea and the surrounding lands determined by waveform modelling: a new database. *J. Geodynamics*, 36, 251-274.

Kiratzi A.A., Karakaisis G.F., Papadimitriou E.F. and Papazachos B.C. (1985): Seismic Source-Parameter Relations for Earthquakes in Greece. *PAGEOPH.*, **123**, 27-41.

Kiratzi A., Wagner G. and Langston C. (1991): Source parameters of some large earthquakes in Northern Aegean determined by body waveform modelling. *PAGEOPH.*, **135**, 515-527.

Kiratzi A., Benetatos C. and Roumelioti Z. (2005): Seismicity and seismotectonic characteristics of ne Aegean Sea and its surrounding lands. *Bull. Geol. Soc. Greece*, **37**, 9-18.

Kockel F. and Mollat H. (1977): *Erläterungen zur Geologischen Karte der Chalkidiki und angrenzender Gebiete 1:100.000 (Nerd Griechenland*. Bundesanstalt für Geowissenschaften und Ruhstoffe, Hannover.

Koral H., Öztürk H. and Hanilçi N. (2009): Tectonically induced coastal uplift mechanism of Gökçeada Island, Northern Aegean Sea, Turkey. *Quatern. Int*., **197**, 43-54.

Koukouvelas I.K. and Aydin A. (2002): Fault structure and related basins of the North Aegean Sea and its surroundings. *Tectonics*, **21**(5), 1046, doi:10.1029/2001TC901037.

Kulhánek O. and Meyer K. (1979): Source Parameters of the Volvi-Langadhas Earthquake of June 20, 1978 deduced from Body-Wave Spectra at Stations Uppsala and Kiruna. *Bull. Geol. Soc. Am.*, 69(4), 1289-1294.

Kurt H., Demirbag E. and Kusçu I. (2000): Active submarine tectonism and formation of the Gulf of Saros, Northeast Aegean Sea, inferred from multi-channel seismic reflection data. *Mar. Geol.*, **165**, 13-26.

Laigle M., Hirn A., Sachpazi M. and Roussos N. (2000): North Aegean crustal deformation: An active fault imaged to 10 km depth by reflection seismic data. Geology, 28, 71-74.

Lybéris N. (1984): Tectonic evolution of the North Aegean trough. *Geol. Soc. London*, Sp. Publ., **17**, 709-725.

Lybéris N. and Sauvage J. (1985): Evolution tectonique de la region nord egeenne (Grece) du Pliocene au Pleistocene. *Bull. Soc. Geol. France*, **8**, I, 4, 581-595.

Maley T.S. and Johnson G.L. (1971): Morphology and structure of the Aegean Sea. Deep-Sea Research, 18, 109-122.

Maravelakis M. (1936): Study on the earthquakes of Chalkidiki (in Greek). Publ. C. Theodoridou, Thessaloniki, 7, 43pp.

Mariolakos I., Zagorchev I., Fountoulis I. and Ivanov M. (2004): Neotectonic Transect Moesia Apulia. Field Trip Guide Book-B26, 32nd Int. Geol. Congr., Pre-Congress Field Trip B26, 72 pp.

Martin L. (1987): *Structure et evolution recente de la mer Egee: Apports d'une etude par seismique reflexion.* Laboratoire de Geodynamique Sous-marine, Villefranche-Sur-Mer, 305 pp.

Mascle J. and Martin L. (1990): Shallow structure and recent evolution of the Aegean Sea: A synthesis based on continuous reflection profiles. *Mar. Geol.*, 94, 271-299.

McKenzie D. (1972): Active Tectonics of the Mediterranean Region. *Geophys. J. R. astr. Soc.*, 30, 109-185.

McNeill L.C., Mille A., Minshull T.A., Bull J.M., Kenyon N.H. and Ivanov M. (2004): Extension of the North Anatolian Fault into the North Aegean Trough: Evidence for transtension, strain partitioning, and analogues for Sea of Marmara basin models. *Tectonics*, **23**, TC2016, doi:10.1029/2002TC001490.

Mercier J.L. (1981): Extensional-compressional tectonics associated with the Aegean Arc: comparison with the Andean Cordillera of south Peru - north Bolivia. *Phil. Trans. R. Soc. Lond. A*, 300, 337-355.

Mercier J.L., Mouyaris N., Simeakis C., Roundoyannis T. and Angelidis C. (1979): Intra-plate deformation: a quantitative study of the faults activated by the 1978 Thessaloniki earthquakes. Nature, 278, 45-48.

Mercier J.-L., Carey E., Mouyaris N., Simeakis K., Roundoyannis T. and Anghelidhis C. (1983): Structural analysis of recent and active faults and regional state of stress in the epicentral area of the 1978 Thessaloniki earthquakes (Northern Greece). *Tectonics*, **2** (6), 577-600.

Mercier J. L., Simeakis K., Sorel D. and Vergely P. (1989): Extensional tectonic regimes in the Aegean basins during the Cenozoic. *Basin Research*, **2**, 49-71.

Meyer B., Armjio R., Massonet D., De Chabalier J.-B., Delacourt C., Ruegg J.-C., Achache C., Briole P. and Papanastassiou D. (1996): The 1995 Grevena (Northern Greece) earthquake: fault model constrained with tectonic observations and SAR interferometry. *Geophys. Res. Lett.*, **23**, 2677-2680.

Meyer B., Armijo R., Massonnet D., de Chabalier J.B., Delacourt C., Ruegg J.C., Achache J. and Papanastassiou D. (1998): Comment on "Geodetic investigation of the 13 May Kozani-Grevena (Greece) earthquake" by Clarke *et al.*, *Geophys. Res. Lett.*, **25**, 129-l30.

Michailidou A., Chatzipetros A. and Pavlides S. (2005): Quantitative analysis - tectonic geomorfology indicators of the faults at the region of Stratoni-Varvara Gomati-M. Panagia in the eastern Chalkidiki. *Bull. Geol. Soc. Greece*, **38**, 14-29.

Mountrakis D. M. and Tranos M.D. (2004): The Kavala-Xanthi-Komotini fault (KXKF): a complicated active fault zone in Eastern Macedonia-Thrace (Northern Greece). 5th Int. Symp. East. Mediter. Geol., Thessaloniki, Greece, 14-20 April 2004, *Proceedings*, S1-19.

Mountrakis D., Kilias A., Pavlides S., Zouros N., Spyropoulos N., Tranos M. and Soulakelis N. (1993a): Field study of the Southern Thessaly highly active Fault Zone. 2nd Congress of the Hellenic Geophysical Union, 5-7 May 1993, Florina, Greece, *Proceedings*, 603-614.

Mountrakis D., Syrides G., Polymenakos L. and Pavlides S. (1993b): The neotectonic structure of the eastern margin of the Axios-Thermaikos depression at the area of western Halkidiki (central Macedonia), *Bull. Geol. Soc. Greece,* **28**(1), 379-395.

Mountrakis D., Kilias A., Pavlides S., Sotiriadis L., Psilovikos A., Astaras Th., Vavliakis E., Koufos G., Dimopoulos G., Soulios G., Christaras V., Skordilis M., Tranos M., Spyropoulos N., Patras D., Syrides G., Lambrinos N. and Laggalis T. (1996a): *Neotectonic map of Greece, Langadhas sheet*. Earthquake Planning and Protection Organisation and European Centre on Prevention and Forecasting of Earthquakes, scale 1:100,000

Mountrakis D., Kilias A., Pavlides S., Sotiriadis L., Psilovikos A., Astaras Th., Vavliakis E., Koufos G., Christaras V., Skordilis M., Tranos M., Spyropoulos N., Patras D., Syrides G., Lambrinos N.

and Laggalis T. (1996b): *Neotectonic map of Greece, Thessaloniki sheet (scale 1:100,000)*. Earthquake Planning and Protection Organisation and European Centre on Prevention and Forecasting of Earthquakes.

Mountrakis D., Pavlides S., Zouros N., Astaras Th. and Chatzipetros A. (1998): Seismic fault geometry and kinematics of the 13 May 1995 western Macedonia (Greece) earthquake. *J. Geodynamics*, **26**(2-4), 175-196.

Mountrakis D., Tranos M., Papazachos C., Thomaidou E., Karagianni E. and Vamvakaris D. (2006): Neotectonic and seismological data concerning major active faults, and the stress regimes of Northern Greece. *Geol. Soc. London*, Sp. Publ. 2006; **260**; 649-670.

Nalbant S.S., Hubert A. and King G.C.P. (1998): Stress coupling between earthquakes in northwest Turkey and the north Aegean Sea. *J. Geophys. Res.J. Geophys. Res.*, **103**, 24469-24486.

North R.G. (1977): Seismic moment, source dimensions, and stress associated with earthquakes in the Mediterranean and Middle East. *Geophys. J. R. astr. Soc.*, **48**, 137-161.

Oliveto A., Mucciarelli M. and Caputo R. (2004): HVSR prospecting in multi-layered environments: An example from the Tyrnavos Basin (Greece). *J. Seismology*, **8**, 395-406.

Palyvos N., Pavlopoulos K., Froussou E., Kranis H., Pustovoytov K., Forman S.L. and Minos‐Minopoulos D. (2010): Paleoseismological investigation of the oblique‐normal Ekkara ground rupture zone accompanying the M 6.7–7.0 earthquake on 30 April 1954 in Thessaly, Greece: Archaeological and geochronological constraints on ground rupture recurrence. *J. Geophys. Res.*, **115**, B06301.

Panagiotopoulos D.G., Papadimitriou E.E., Papaioannou Ch.A., Scordilis E.M. and Papazachos B.C. (1993): Source Properties of the 21 December 1990 Goumenissa Earthquake in Northern Greece. 2nd Congress of the Hellenic Geophysical Union, 5-7 May 1993, Florina, Greece, *Proceedings*, 286-296.

Papadimitriou E.E and Sykes L.R. (2001): Evolution of the stress field in the northern Aegean Sea (Greece). *Geophys. J. Int.*, **146**, 747-759.

Papadimitriou P., Voulgaris N., Kassaras I., Kaviris G., Delibasis N. and Makropoulos K. (2002): The Mw = 6.0, 7 September 1999 Athens Earthquake. *Natural Hazards*, **27**, 15-33.

Papadopoulos G.A. (1992): Rupture zones of strong earthquakes in the Thessalia region, Central Greece. *Proc. XXIII Gen. Assembly Europ. Seismol Commission*, Prague, September 2, 1992, **2**, 337-340.

Papadopoulos G.A. (2000): *Historical earthquakes and tsunamis in the Corinth Rift, Central Greece*. National Observatory of Athens, Institute of Geodynamics, Publ. n. 12, pp.128, Athens.

Papanastassiou D. (2001): The Konitsa, Epirus-NW Greece, July 26 (Ms = 5.4) and August 5, 1996, (Ms = 5.7) earthquakes sequence. *Bull. Geol. Soc. Greece*, **34**(4), 1555-1562.

Papanikolaou I.D. and Papanikolaou D.I. (2007): Seismic hazard scenarios from the longest geologically constrained active fault of the Aegean. *Quaternary International*, **171-172**, 31-44.

Papanikolaou D., Alexandri M., Nomikou P. and Ballas D. (2002): Morphotectonic structure of the western part of the North Aegean Basin based on swath bathymetry. *Mar. Geol.Mar. Geol.*, **190**, 465-492.

Papanikolaou D., Alexandri M. and Nomikou P. (2006): Active faulting in the North Aegean basin. In: Dilek Y. and Pavlides S. (eds.), Postcollisional Tectonics and Magmatism in the Mediterranean Region and Asia. *Geol. Soc. Am.*, Special Paper **409**, 189-20.

Papastamatiou D. and Mouyiaris N. (1986): The Sophadhes earthquake occurred on April 30th 1954 – field observations by Yannis Papastamatiou, Geol. & Geoph. Res., Sp. Issue, 341-362

Papazachos B.C. (1990): Seismicity of the Aegean and surrounding area. *Tectonophysics*, **178**, 287-308.

Papazachos B. and Papazachou C. (1997): *The earthquakes of Greece.* Second edition, Editions ZITI, Thessaloniki, 304 pp.

Papazachos B., Mountrakis D., Psilovikos A. and Leventakis G. (1979): Surface fault traces and fault plane solutions of the May-June 1978 major shocks in the Thessaloniki area, Greece. *Tectonophysics*, 53, 171-183.

Papazachos B.C., Panagiotopoulos D.G., Tsapanos T.M., Mountrakis D.M. and Dimopoulos G.Ch. (1983): A study of the 1980 summer seismic sequence in the Magnesia region of Central Greece. *Geophys. J. R. astr. Soc.*, **75**, 155-168.

Papazachos B.C., Kiratzi A.A., Voidomatis P. and Papaioannou C.A. (1984): A study of the December 1981 - January 1982 seismic activity in Northern Aegean Sea. *Boll. Geofis. Teor. Appl.*, **26**(101-102), 101-113.

Papazachos B., Kiratzi A. and Papadimitriou E. (1991): Regional Focal Mechanisms for Earthquakes in the Aegean Area. *PAGEOPH*, **136**(4), 405-420.

Papazachos B.C., Karakostas B.G., Kiratzi A.A., Papadimitriou E.E. and Papazachos C.B. (1998): A model for the 1995 Kozani-Grevena seismic sequence. *J. Geodyn.*, **26**, 217-231.

Papazachos B.C., Comninakis P.E., Scordilis E.M., Karakaisis G.F. and C.B. Papazachos (2009): A catalogue of earthquakes in the Mediterranean and surrounding area for the period 1901-Sep. 2009, Publ. Geophys. Laboratory, Aristotle University of Thessaloniki, http://geophysics.geo.auth.gr (last visited 21/01/2011) .

Paradisopoulou P.M., Karakostas V.G., Papadimitriou E.E., Tranos M.D., Papazachos C.B. and Karakaisis G.F. (2004): Microearthquake study of the broader Thessaloniki area. 5th Int. Symp. East. Mediter. Geol., 14-20 April 2004, Thessaloniki, Greece, *Proceedings*, **2**, 623-626.

Paradisopoulou P.M., Karakostas V.G., Papadimitriou E.E., Tranos M.D., Papazachos C.B. and Karakaisis G.F. (2006): Microearthquake study of the broader Thessaloniki area (Northern Greece). *Ann. Geoph.*, **49**(4/5), 1081-1093.

Pavlides S. (1985): *Neotectonic evolution of the Florina-Vegoritis-Ptolemais basin (W. Macedonia, Greece)*. Ph.D. Thesis, University of Thessaloniki, Greece, 265 pp.

Pavlides S. (1993): Active faulting in multi-fractured seismogenic areas; examples from Greece, *Z. Geomorph. N.F.*, **94**, 57-72.

Pavlides S.B. (1998): Dating the neotectonisms in south Almopias (Central Macedonia, N. Greece). *Bull. Geol. Soc. Greece*, **32**(1), 189-197.

Pavlides S. and Caputo R. (1994): The North Aegean region: a tectonic paradox? *Terra Nova*, **6**, 37-44.

Pavlides S. and Caputo R. (2004): Magnitude versus faults' surface parameters: quantitative relationships from the Aegean *Tectonophysics*, **380**, 159-188.

Pavlides S.B. and Kilias A.A. (1987): Neotectonic and active faults along the Serbomacedonian zone (SE Chalkidiki, northern Greece). *Ann. Tectonicae*, **1**(2), 97-104.

Pavlides S.B. and Mountrakis D.M. (1987): Extensional tectonics of northwestern Macedonia, Greece, since the late Miocene. *J. Struct. Geol.*, **9**(4), 385-392.

Pavlides S. and Simeakis K. (1987/88): Neotectonics and active tectonics in low seismicity areas of Greece: Vegoritis (NW Macedonia) and Melos isl complex (Cyclades) - comparison. *Ann. Géol. Pays Helléniques*, **33**(2), 161-176.

Pavlides S.B. and Tranos M.D. (1991): Structural characteristics of two strong earthquakes in the North Aegean: Ierissos (1932) and Agios Efstratios (1968). *J. Struct. Geol.*, **13**, 205-214.

Pavlides S., Mountrakis D., Kilias A. and Tranos M. (1990): The role of strike-slip movements in the extensional area of Northern Aegean (Greece). A case of transtensional tectonics. *Ann. Tectonicae*, **4**(2), 196-211.

Pavlides S.B., Zouros N.C., Chatzipetros A.A., Kostopoulos D.S. and Mountrakis D.M. (1995): The 13 May 1995 western Macedonia, Greece (Kozani Grevena) earthquake; preliminary results. *Terra Nova*, **7**, 544-549.

Pavlides S., Papadopoulos G.A. and Ganas A. (2002): The fault that caused the Athens September 1999 Ms 5.9 earthquake: field observations. *Nat. Hazards,* **27**(1-2), 61-84.

Pavlides S., Chatzipetros A. and Tsapanos Th. (2004a): The Kerkini-Sidirokastro (northern Strymon valley, Greece) active fault and its seismic potential. 4th National Geoph. Conf., 4-5 October 2004, Sofia, *Abstracts*.

Pavlides S., Kouskouna V. Ganas A., Caputo R., Karastathis V. and Sokos E. (2004b): The Gonnoi (NE Thessaly - Greece) earthquake (June 2003, Ms=5.5) and the neotectonic regime of Lower Olympus. Int. Symp. Eastern Mediterranean Geology, 14-20 April 2004, Thessaloniki, Greece, *Proceedings*, **2**, 627-630.

Pavlides S., Valkaniotis S., Kurcel A., Papathanassiou G. and Chatzipetros A. (2005): Neotectonics of Samothraki Island (NE Aegean, Greece) in relation to the North Anatolian Fault. *Bull. Geol. Soc. Greece*, **37**, 19-28.

Pavlides S., Tsapanos T., Zouros N., Sboras S., Koravos G. and Chatzipetros A. (2009): Using Active Fault Data for Assessing Seismic Hazard: A Case Study from NE Aegean Sea, Greece. XVIIth Int. Conf. Soil Mech. & Geotechn. Eng., 2-3 October 2009, Alexandria, Egypt.

Pavlides S., Caputo R., Sboras S., Chatzipetros A., Papathanasiou G. and Valkaniotis S. (2010): The Greek Catalogue of Active Faults and Database of Seismogenic Sources. *Bull. Geol. Soc. Greece*, **43**(1), 486-494.

Perissoratis C., Angelopoulos I. and Mitropoulos D. (1991): Surficial Sediment Map of the Aegean Sea Floor: Pagasitikos Sheet, scale 1:200 000, IGME editions, Athens.

Psilovikos A. (1984): Geomorphological and structural modification of the Serbomacedonian massif during the neotectonic stage. *Tectonophysics*, 110**,** 27-45.

Psilovikos A. and Papaphilippou E. (1990): Pediments, alluvial fans and neotectonic movements of the Mt Kerkini/Belassitsa. Geologica Rhodopica, 2, Aristotle University Press, Thessaloniki, 95-103.

Resor P.G., Pollard D.D., Wright T.J. and Beroza G.C. (2005): Integrating high-precision aftershock locations and geodetic observations to model coseismic deformation associated with the 1995 Kozani-Grevena earthquake, Greece. *J. Geophys. Res.*, **110**, B09402.

Rigo A., de Chabalier J.-B., Meyer B. and Armijo R. (2004): The 1995 Kozani-Grevena (northern Greece) earthquake revisited: An improved faulting model from synthetic aperture radar interferometry. *Geophys. J. Int.*, **157**, 727-736.

Rocca A.C., Karakaisis G.F., Karacostas B.G., Kiratzi A.A., Scordilis E.M. and Papazachos B.C. (1985): Further evidence on the strike-slip faulting of the Northern Aegean Trough based on properties of the August-November 1983 seismic sequence. *Boll. Geofis. Teor. Appl.*, **XXVII**(106), 101-109.

Rockwell T., Barka A., Dawson T., Akyuz S. and Thorup K. (2001): Paleoseismology of the Gazikoy-Saros segment of the North Anatolia fault, northwestern Turkey: Comparison of the historical and paleoseismic records, implications of regional seismic hazard, and models of earthquake recurrence. *J. Seismol.*, **5**, 433-448.

Rondoyanni Th., Georgiou Ch., Galanakis D. and Kourouzidis M. (2004): Evidences of active faulting in Thrace region (Northeastern Greece). *Bull. Geol. Soc. Greece*, **36**, 1671-1678.

Roumelioti Z., Theodulidis N. and Kiratzi A. (2007): The 20 June 1978 Thessaloniki (Northern Greece) earthquake revisited: Slip distribution and forward modeling of geodetic and seismological observations. 4th Int. Conf. Earthq. Geotech. Eng., June 25-28, Paper No. 1594.

Roussos N and Lyssimachou T. (1991): Structure of the Central North Aegean Trough: an active strike-slip deformation zone. *Basin Research*, **3**, 39-48.

Saatçilar R., Ergintav S., Demirbag E. and Inan S. (1999): Character of active faulting in the North Aegean Sea. *Mar. Geol.*, **160**, 339-353.

Sakellariou D., Roussakis G., Kranis C., Kamberi E., Georgiou P. and Skoulikidis N. (2001): Neotectonic Movements, Sedimentation and Water-Level Fluctuation of the Lake Vegoritis in Upper Quaternary. *Bull. Geol. Soc. Greece*, **34**(1), 207-216.

Sboras S and Caputo R. (2010): Possible occurrence of low-angle normal faults in Central and Northern Greece. 29° Convegno Nazionale di GNGTS, 26-28 October 2009, Prato, Italy, *Extended Abstracts*, 126-128.

Soufleris Ch. and King G. (1983): A source study of the largest foreshock (on May 23) and the mainshock (on June 20) of the Thessaloniki 1978 earthquake sequence. In: Papazachos, B.C. and P.G. Carydis (eds.), *The Thessaloniki, Northern Greece, earthquake of June 20, 1978 and its seismic sequence*, Technical Chamber of Greece, 201-222.

Soufleris C. and Stewart G. (1981): A source study of the Thessaloniki (northern Greece) 1978 earthquake sequence. *Geophys. J. R. astr. Soc.*, **67**, 343-358.

Soufleris C., Jackson J.A., King G.C.P., Spencer C.P. and Scholz C.H. (1982): The 1978 earthquake sequence near Thessaloniki (northern Greece). *Geophys. J. R. astr. Soc.*, **68**, 429-458.

Stiros S.C. (1998). Historical seismicity, paleoseismicity and seismic risk in Western Macedonia, Northern Greece. *J. Geodyn.,* **26**(2-4), 271-287.

Stiros S.C. and Drakos A. (2000): Geodetic constrains on the fault pattern of the 1978 Thessaloniki (Northern Greece) earthquake (Ms=6.4). *Geophys. J. Int.*, **143**, 679-688.

Stiros S., Triantafillides P. and Chasapis A. (2004): Geodetic evidence for active uplift of the Olymbus Mt., Greece. *Bull. Geol. Soc. Greece*, **36**(4), 1697-1705.

Suhadolc P., Moratto L., Costa G. and Triantafyllidis P. (2007): Source Modeling of the Kozani and Arnea 1995 Events with Strong Motion Estimates for the City of Thessaloniki. J. Earthq. Eng., **11**(4), 560-581.

Taymaz T., Jackson J. and McKenzie D. (1991): Active tectonics of the north and central Aegean Sea. *Geophys. J. Int.*, **106**, 433-490.

Tranos M.D. (1998): *Contribution to the study of the neotectonic deformation in the region of Central Macedonia and North Aegean*. PhD thesis, Aristotle University of Thessaloniki, pp. 349

Tranos M.D. and Mountrakis D.M. (2004): The Serres fault zone (SZF): an active fault zone in Eastern Macedonia (Northern Greece). 5th Int. Symp. East. Mediter. Geol., Thessaloniki, Greece, 14-20 April 2004, *Proceedings*, S1-18.

Tranos M., Papadimitriou E. and Kilias A. (2003): Thessaloniki-Gerakarou Fault Zone (TGFZ): the western extension of the 1978 Thessaloniki earthquake fault (Northern Greece) and seismic hazard assessment. *J. Struct. Geol.*, **25**, 2109-2123.

Tselentis G.-A., Sokos E., Martakis N. and Serpetsidaki A. (2006): Seismicity and Seismotectonics in Epirus, Western Greece: Results from a Microearthquake Survey, *Bull. Seism. Soc. Am.*, **96**(5), 1706-1717.

Tüysüz O., Barka A., Yigitbas E. (1998): Geology of the Saros graben and its implications for the evolution of the North Anatolian fault in the Ganos-Saros region, northwestern Turkey. *Tectonophysics*, 293, 105-126.

Ustaömer T., Gökaşan E, Tur H., Görüm T, Batuk F.G, Kalafat D., Alp H., Ecevitoğlu B. and Birkan H. (2008): *Geo-Mar. Lett.*, **28**, 171-193.

Valensise G. and Pantosti D. (Eds) (2001): Database of potential sources for earthquakes larger than M 5.5 in Italy. *Ann. Geofisica*, **44**(4), 797-807.

Vannucci G. and Gasperini P. (2003): A database of revised fault plane solutions for Italy and surrounding regions. *Computers & Geosciences*, **29**, 903-909.

Vannucci G. and Gasperini P. (2004): The new release of the database of Earthquake Mechanisms of the Mediterranean Area (EMMA Version 2). *Ann. Geofis.*, supplement to Vol. **47**, 307-334.

Voidomatis P. (1989): Some aspects of a seismotectonic synthesis in the North Aegean Sea and surrounding area. *Boll. Geofis. Teor. Appl.*, **31**, 49-61.

Vougioukalakis G. (2002): *Petrological, Geochemical and Volcunological study of the Almopias Pliocene volcanic formations and their correlation with the geothermal manifestations in the area*. PhD Thesis, Aristotle University of Thessaloniki, 303 pp.

Wells D.L. and Coppersmith J.K. (1994): New Empirical Relationships among Magnitude, Rupture Length, Rupture Width, Rupture Area, and Surface Displacement. *Bull. Seism. Soc. Am.*, **84**, 974-1002.

Yaltirak C. and Alpar B. (2002): Kinematics and evolution of the northern branch of the North Anatolian Fault (Ganos Fault) between the Sea of Marmara and the Gulf of Saros. *Mar. Geol.*, **190**, 351-366.

Yaltirak C., Alpar B. and Yüce H. (1998): Tectonic elements controlling the evolution of the Gulf of Saros (northeastern Aegean Sea, Turkey). *Tectonophysics*, **300**, 227-248.

Zervopoulou A. (2004): *Preliminary Report of the active and possible active faults of the broader area of the city of Thessaloniki which will affect the urban area during a probable reactivation (in Greek).* Report Department of Geology, Aristotle University of Thessaloniki, Greece, 35 pp.

Zervopoulou A. (2009). *Neotectonic faults of the broader Thessaloniki area in association with foundation soils (in Greek with English abstract).* PhD Thesis, Department of Geology, Aristotle University of Thessaloniki, Greece, 300 pp.

Zervopoulou A. and Pavlides S. (2005): Morphotectonic study of the broader area of Thessaloniki for the cartography of neotectonic faults. *Bull. Geol. Soc. Greece*, **38**, 30-41.

Zervopoulou A., Chatzipetros A., Tsiokos L., Syrides G. and Pavlides S. (2007): Non-seismic surface faulting: the Peraia Fault case study (Thessaloniki, N. Greece). 4th International Conference on Earthquake Geotechnical Engineering, June 25-28, 2007, Paper No. 1610.

Zovoili E., Konstantinidi E. and Koukouvelas I.K. (2004): Tectonic geomorphology of escarpments: the cases of Kompotades and Nea Anchialos Faults. *Bull. Geol. Soc. Greece*, **36**, 1716-1725.

Figure captions

Fig. 1: Map of the seismogenic sources recognized in the Northern Aegean region and included at present in GreDaSS. ISS: individual seismogenic sources; CSS: composite seismogenic sources; DSS: debated seismogenic sources.

Fig. 2: (top) Historical (from Papazachos and Papazacou, 1997) and (bottom) instrumental (National Observatory of Athens) seismicity in the Northern Aegean region.

Fig. 3: The seismogenic sources belonging to the "northern Greece fault belt" with the major events discussed in the text. Symbols of seismogenic sources as in figure 1; see figure 2 for magnitudes scale.

Fig. 4: The seismogenic sources belonging to the "Chalkidiki fault system" with the major events discussed in the text. Symbols of seismogenic sources as in figure 1; see figure 2 for magnitudes scale.

Fig. 5: The seismogenic sources belonging to the "anti-Hellenides fault system" with the major events discussed in the text. Symbols of seismogenic sources as in figure 1; see figure 2 for magnitudes scale.

Fig. 6: The seismogenic sources belonging to the "North Aegean offshore fault system" with the major events discussed in the text. Symbols of seismogenic sources as in figure 1; see figure 2 for magnitudes scale.

Fig. 7: The seismogenic sources belonging to the "Thessalian fault system" with the major events discussed in the text. Symbols of seismogenic sources as in figure 1; see figure 2 for magnitudes scale.

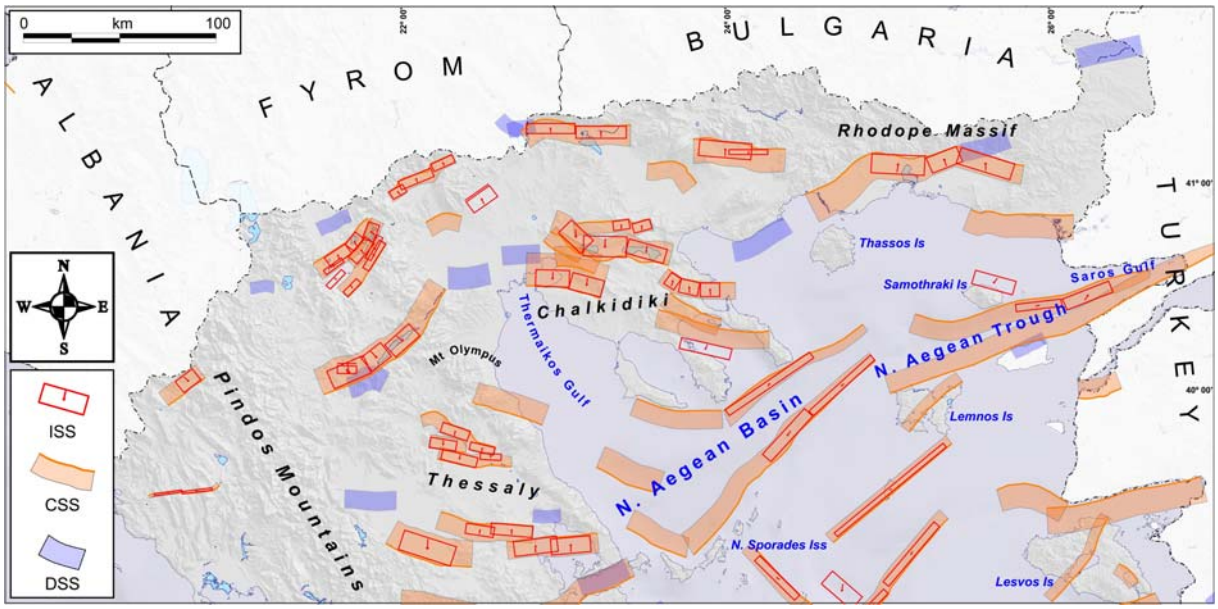
0
km
100
N
W
E
S
ISS
CSS
DSS
ALBANIA
FYROM
BULGARIA
TURKEY
Rhodope Massif
Thassos Is
Samothraki Is
Saros Gulf
Chalkidiki
Thermaikos Gulf
Mt Olympus
N. Aegean Trough
N. Aegean Basin
Lemnos Is
Pindos Mountains
Thessaly
N. Sporades Iss
Lesvos Is

Fig. 1

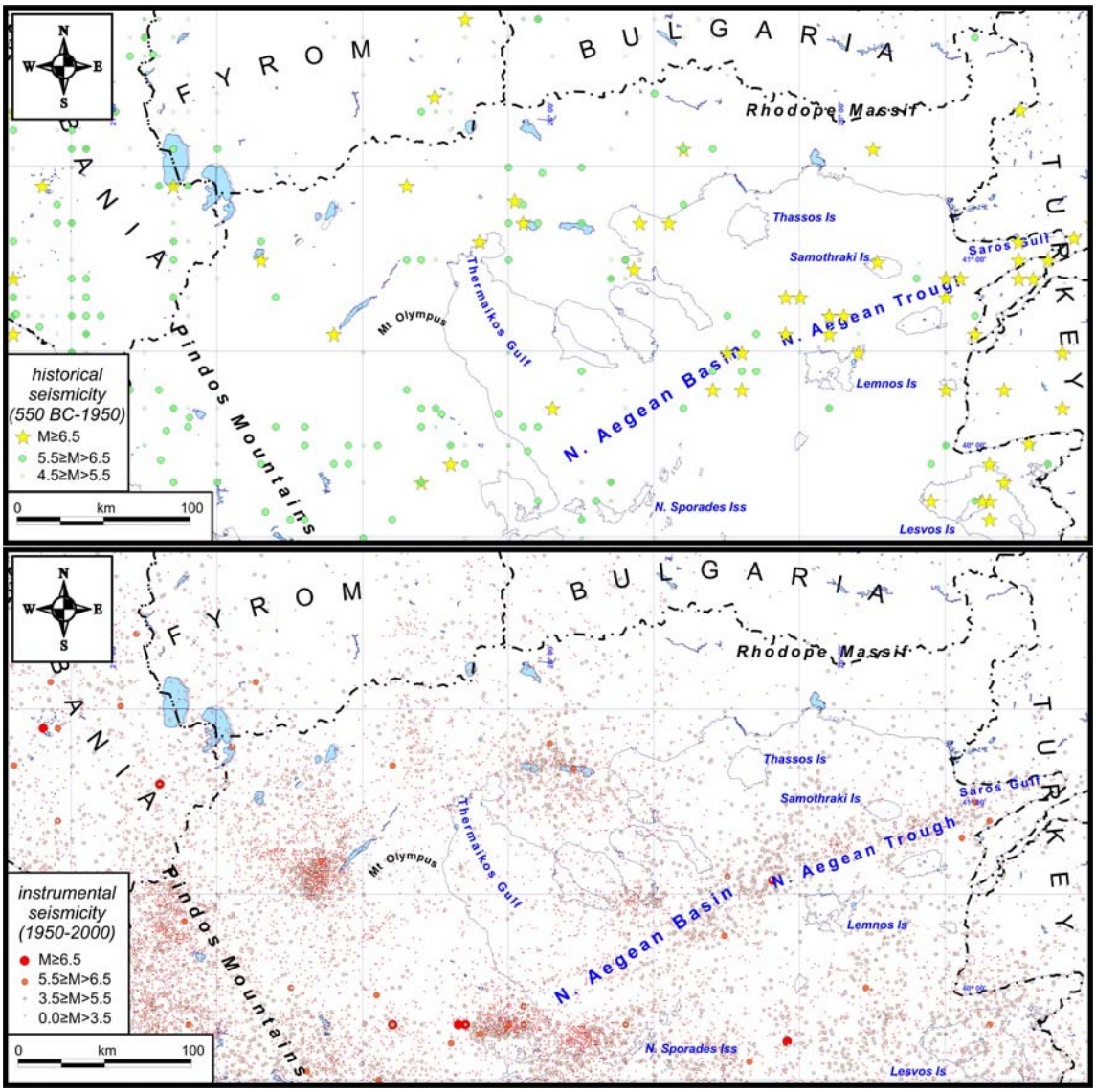
F Y R O M
B U L G A R I A
Rhodope Massif
T U R K E Y
Thassos Is
Samothraki Is
Saros Gulf
Mt Olympus
Thermaikos Gulf
N. Aegean Trough
N. Aegean Basin
Lemnos Is
N. Sporades Iss
Lesvos Is
Pindos Mountains
historical seismicity (550 BC-1950)
M≥6.5
5.5≥M>6.5
4.5≥M>5.5
0 km 100
instrumental seismicity (1950-2000)
M≥6.5
5.5≥M>6.5
3.5≥M>5.5
0.0≥M>3.5
0 km 100

Fig. 2

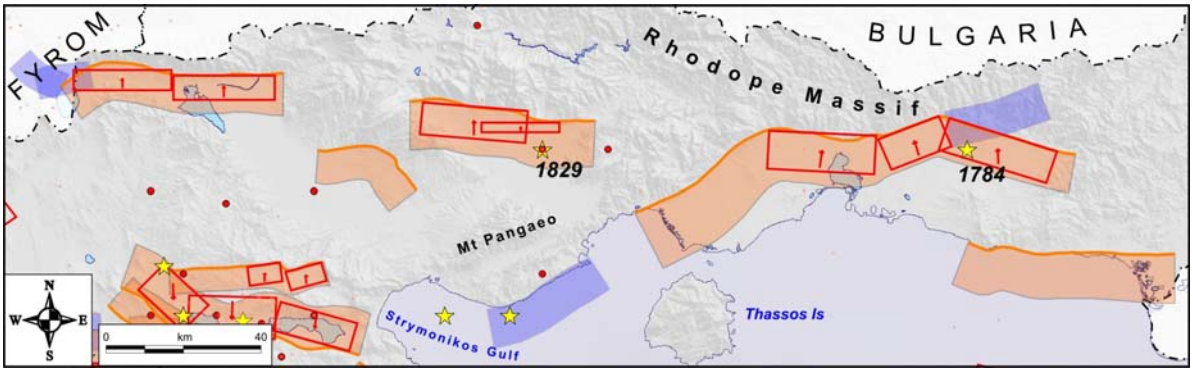

Fig. 3

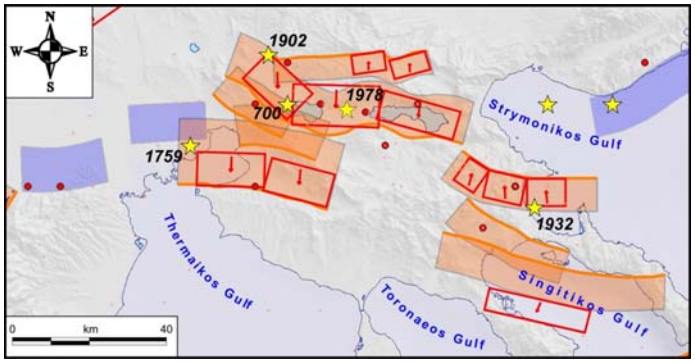

Fig. 4

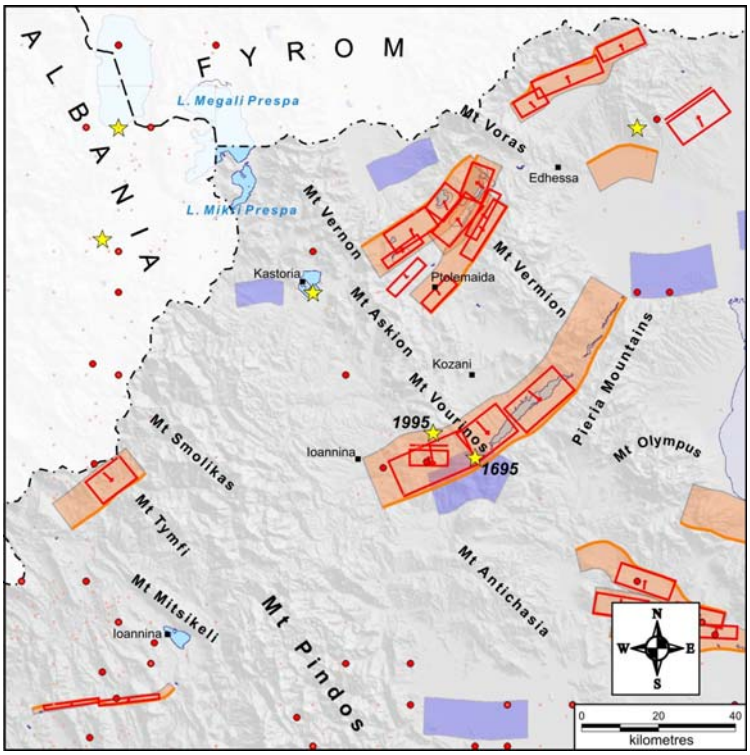

Fig. 5

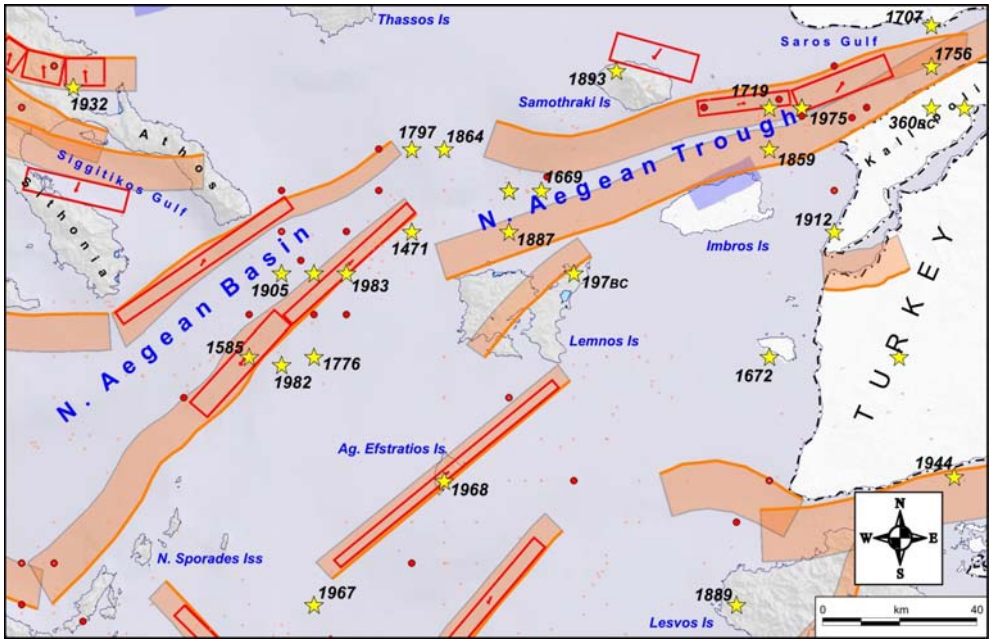
Thassos Is
Saros Gulf
1707
1756
1893
1932
Samothraki Is
1719
1975
360BC
Athos
Sithonia
Siggitikos Gulf
1797
1864
N. Aegean Trough
1859
1669
1912
1887
Imbros Is
1471
N. Aegean Basin
1905
1983
197BC
Lemnos Is
1585
1776
1982
1672
TURKEY
Ag. Efstratios Is
1944
1968
N. Sporades Iss
1967
1889
Lesvos Is
N
W
E
S
0
km
40

Fig. 6

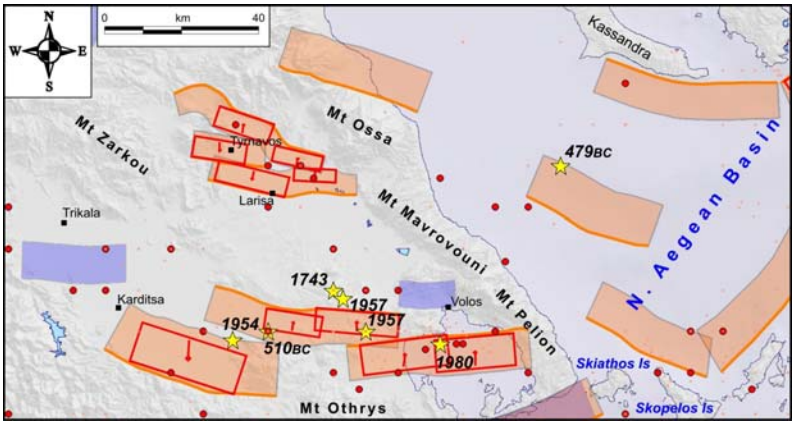
N
W
E
S
0
km
40
Kassandra
Mt Ossa
Mt Zarkou
Tyrnavos
Larisa
Trikala
479BC
Mt Mavrovouni
N. Aegean Basin
1743
Karditsa
1957
1957
Volos
Mt Pelion
1954
510BC
1980
Skiathos Is
Mt Othrys
Skopelos Is

Fig. 7